Article

Maltose Utilization as a Novel Selection Strategy for Continuous Evolution of Microbes with Enhanced Metabolite Production

Shu-De Liu, Yi-Nan Wu, Tian-Min Wang, Chong Zhang, and Xin-Hui Xing

ACS Synth. Biol., **Just Accepted Manuscript** • DOI: 10.1021/acssynbio.7b00247 • Publication Date (Web): 25 Aug 2017

Maltose Utilization as a Novel Selection Strategy for Continuous Evolution of Microbes with Enhanced Metabolite Production

Shu-De Liu[1,2], Yi-Nan Wu[1,2], Tian-Min Wang, Chong Zhang*[,1], Xin-Hui Xing[1]

[1]MOE Key Laboratory for Industrial Biocatalysis, Department of Chemical Engineering, Center for Synthetic & Systems Biology, Tsinghua University, Beijing, China

[2]These authors contributed equally to the work

*Corresponding author, Chong Zhang: chongzhang@tsinghua.edu.cn

ABSTRACT

We have developed a novel selection circuit based on carbon source utilization that establishes and sustains growth-production coupling over several generations in a medium with maltose as the sole carbon source. In contrast to traditional antibiotic resistance–based circuits, we first approved that coupling of cell fitness to metabolite production by our circuit was more robust with a much lower escape risk even after many rounds of selection. We then applied the selection circuit to the optimization of L-tryptophan (L-Trp) production. We demonstrated that it enriched for specific mutants with increased L-Trp productivity whether applied to a small defined, or a relatively large and undefined, mutational library. From the latter, we identified four novel mutations with enhanced L-Trp output. Finally, we used it to select for several high L-Trp producers with randomly generated genome-wide mutations and obtained strains with up to 65% increased L-Trp production. This selection circuit provides new perspectives for the optimization of microbial cell factories for diverse metabolite production and the discovery of novel genotype-phenotype associations at the single-gene and whole genome levels.

KEY WORDS: adaptive laboratory evolution, biosensor, maltose utilization, pathway optimization, L-tryptophan biosynthesis

INTRODUCTION

In the past two decades, adaptive laboratory evolution (ALE) has been widely used in the field of metabolic engineering as a strategy to accelerate microbial evolution to obtain industrially relevant phenotypes.[1,2] ALE-generated phenotypes have included the ability to utilize non-native substrates,[3] tolerance to fermentation products,[4] increased growth under specific environmental conditions,[5] optimal balance between product formation and biomass generation,[6] and increased productivity, titer, and yield of target product.[7] Compared with rational metabolic engineering, ALE as a strain-optimization strategy has the advantage of allowing non-intuitive beneficial mutations to be enriched, thereby exceeding the scope of

available knowledge about metabolic systems and microorganism physiology.[8] Recent advances in the generation of genotypic diversity have also accelerated the application of ALE and increased the possibility of producing desired phenotypes through ALE.[9–11]

Most ALE applications to date have focused on fitness phenotypes because there are no general methods available to couple metabolite production to cellular fitness, e.g., to universally apply the ALE strategy directly to optimize strains for metabolite production. Although a study using ALE recently succeeded in improving carotenoid production in *Saccharomyces cerevisiae* under oxidative stress by exploiting the antioxidant properties of carotenoids,[12] most metabolites are not easily coupled to cellular fitness. To solve this problem, research is underway to transform the product signal into cellular fitness by applying synthetic genetic circuits. In these circuits, engineered biosensor responded to the metabolite concentration and controlled the expression of downstream fitness-coupled parts, such as antibiotic resistance genes.[13,14] However, this strategy is susceptible to mutation of bacteria, termed escapees[15] that recovered normal growth via spontaneous mutations that defeated the stressed conditions. These escapees formed competing populations with undesired phenotypes, impeding the enrichment of desired mutants with improved chemical production. To address this issue, two compromising strategies have been adopted. In the first, the engineered genotypic diversity was constructed into plasmid-based selection circuits, and bacterial strains carrying the constructs are subjected to selection. To avoid escapees, the plasmids are extracted from the evolved strains after several rounds of selection and retransformed into the starting parent strain for further selection.[13] In an alternative approach, a negative selection is used to eliminate escapees via a toggled negative selection phase.[14] The former approach severely impedes the continuity of the evolution process whereas the latter reduces the efficiency of selection, which results in wasted time and higher costs. Moreover, to avoid rapid generation of escapees, both systems rely on the predefined synthetic mutation library, the genotype space sampling limitation of which contradicts the

fundamental purpose of ALE of finding unknown loci related to targeted phenotypes.

Herein, we propose a novel selection strategy based on specific carbon source utilization rather than lethal substances to meet the requirements of continuous evolution with low risk of generating escapees. We designed a plasmid-based genetic circuit, in which the expression of a maltose-utilizing enzyme (amylomaltase) is under the control of a biosensor of a target metabolite. Our reasoning was as follows: First, when present in a strain that is deficient for the maltase, the ability to utilize maltose as the sole carbon source becomes dependent on the target metabolite; thus tightly coupling production and growth. Second, adaptation of microbes to the selective pressure imposed by inherently non-exploitable carbon sources (e.g., maltose) is likely considerably rarer than to the stress generated by antibiotics. Based on these two assumptions, we hypothesized that this circuit-based strategy would significantly reduce the possibility of escapee emergence during the selection process and thereby render continuous evolution possible.

In this study, we chose L-tryptophan (L-Trp) as our target metabolite and constructed a genetic circuit based on a L-Trp biosensor. L-Trp sensing mechanism we used is firstly revealed in transcriptional regulation of the tnaCAB operon based on the nascent leader peptide mechanism (encoded in tnaC).[16] In our previous work, we firstly repurposed this naturally occurring mechanism as a biosensor by fusing reporter gene GFP downstream to the regulatory element (from 24-bp upstream of *tnaC* to 30-bp downstream of the *tnaA* start codon). The expression of reporter genes was linearly dependent on the concentration of L-Trp in operational range.[17] Here, we fused the regulatory element with *malQ*, the gene encoding amylomaltase,[18] downstream of the L-arabinose induced pBAD promoter to achieve growth-production coupling and selection of desired phenotypes (Figure 1a). By replacing *malQ* with *tetA* that confers tetracycline resistance, we also constructed a control circuit to compare the anti-escape ability of a traditional antibiotics-based strategy with this novel approach. We demonstrated that, for both circuits, cell growth

positively responded to exogenously added L-Trp, and strains with high L-Trp production were enriched within days by simply transferring the culture under the appropriate selective environment. However, the kinetics of the two systems were quite different: using a carbon source as selection pressure was much more robust with fewer escapees even after 30 days of evolution, whereas tetracycline (tet) resistance rapidly emerged after just 2 days. We then applied this new selection method to select for high L-Trp producers from two types of *TrpE* mutant libraries—a site-saturation mutagenesis library and a mutant library generated by error-prone PCR. *TrpE* encodes anthranilate synthase, or TrpE, a rate-limiting enzyme in the L-Trp biosynthetic pathway.[19] We successfully enriched for new beneficial mutations during the continuous selection process. We also applied our selection strategy to a mutational library with random mutations at the genome level and successfully enriched strains with increased L-Trp production of up to 65% by a series of continuous selections. This experimental selection strategy enabled the efficient enrichment of desired phenotypes continuously with very low risk of generating evolution-induced escapees based on either gene level synthetic library or genome level spontaneous mutation library. This strategy may be extended as a universal and powerful tool for the optimization of microbial production of desired metabolites. Furthermore, it provides a new avenue for the discovery of genotype-phenotype associations by identifying the determinative genetic elements for the targeted genotype in a quick and relatively high-throughput manner.

RESULTS AND DISCUSSION

Establishment and Characterization of the Growth-based Selection Platform. To realize growth-production coupling, we constructed a selection circuit, pMC, by expressing *malQ*, encoding a maltose hydrolase, downstream of the L-Trp biosensor in a medium copy–number plasmid, pTrc99A. In this circuit, the L-Trp biosensor activates the transcription of *malQ* by positively responding to the intracellular concentration of L-Trp. So, intracellular L-Trp can activate the expression

of the maltose hydrolase, which hydrolyzes maltose to yield glucose—the carbon source that is readily utilized by microbes for growth (Figure 1a). Thus, we predicted that by culturing microbes harboring the pMC circuit in medium with maltose as the sole carbon source, a high L-Trp–producing bacterium would grow faster than a relatively low L-Trp–producing competitor; hence, the former would ultimately predominate in the population as transfer culture continued, enabling the high-throughput growth-based selection (Figure 1a).

To validate the function of the pMC circuit in growth-production coupling, we cultured strain B1 (E. coli BL21(DE3) *ΔmalQ ΔaraA,* in which *araA* was deleted to make sure the host can't utilize the inducer L-arabinose for growth) harboring the pMC circuit in the M9 culture medium, which contained maltose as the sole carbon source and different concentrations of exogenously added Ala-Trp dipeptide. It has been proved that dipeptide addition is a valid method to increase the cytosolic pool of a specific amino acid in *E.coli*.[20] After membrane transport, expedited by alanine residue, the Ala-Trp dipeptide can be hydrolyzed into L-Ala and L-Trp, and make intracellular L-Trp concentration linearly dependent on the extracellular dipeptide concentration.[17] Additionally, we observed the direct addition of L-Trp moderately inhibited cell growth. Therefore, we used Ala-Trp to control the intracellular concentration of L-Trp in our work. We found that strains in the high Ala-Trp environments grew faster than those in low Ala-Trp environments, and the trend continued up to a concentration of 20 μM Ala-Trp (Figure 1b). For Ala-Trp concentrations >20 μM, much lower than 600 μM (upper detection limit of L-Trp biosensor quantified by expressing *sfGFP* downstream of the *malQ* and detecting the Ala-Trp induced fluorescence response in non-selective medium) (Figure S1), the growth of the strains remained unchanged, possibly because the amount of maltose hydrolase expressed was sufficient to hydrolyze maltose to glucose for growth. It is reasonable that strains grown in media that contained glucose as the sole carbon source had the highest growth rates as they directly utilized glucose for growth with no burden of expressing maltose hydrolase and no lag time for transforming maltose

to glucose. The strain still survived in medium without Ala-Trp, although with a relatively low growth rate, and this may have resulted from leaky expression of *malQ*. And the strain without the pMC circuit (NC) hardly survived in the medium. According to our preliminary experiments to culture strain under the same condition as NC, it showed no cell growth for as long as 30 days (data not shown). To further verify the difference in growth rates that resulted from different maltose-utilizing abilities, we used HPLC to measure the maltose concentration in the media during culture. We found that the difference in maltose consumption rate in response to Ala-Trp concentration exhibited the same trend as the growth rate (Figure S2). In short summary, this result confirmed that the pMC selection circuit coupled the growth of the microbes to L-Trp based on the conversion of maltose to glucose, specifically through L-Trp–induced expression of *malQ*.

We reasoned that during the selection process, strains with high production would be enriched among the mixture of strains with different production. As proof of concept, we focused on *TrpED*, the bottleneck step in L-Trp biosynthesis[19] and sought to engineer *TrpED* to construct a series of mutant strains with different L-Trp production. The *TrpED* encodes anthranilate synthase. This enzyme catalyzes the reaction of chorismate to L-Trp and are feedback-inhibited by intracellular L-Trp, the removal of which significantly increases chorismate-to- L-Trp flux. In addition to the wild-type *TrpED*, we expressed a mutated form, $TrpE^{fbr}D$, in which sensitivity to feedback inhibition was eliminated by two point mutations, Met293Thr and Ser40Phe. Based on the previous reported B8 strain (*E. coli* BL21(DE3) Δ*tnaA* Δ*TrpR* Δ*pheA*) optimized for L-Trp production[19], we further deleted *araA* and *malQ* to construct B10 strain as the host for this assay. The strain B10/pEDfbr, which expressed mutated $TrpE^{fbr}D$, had a higher L-Trp titer/OD ~18 mg/L/OD, whereas strain B10/pEDwt, which expressed wild-type *TrpED*, had a titer/OD of only 1 mg/L/OD (Figure S3). We then transferred the pMC circuit into each of these strains to produce B10/pMC+pEDwt and B10/pMC+pEDfbr and cultured the two strains in both M9-cas-maltose (selective) and M9-cas-glucose (non-selective) media. As anticipated,

only in the selective medium did B10/pMC+pEDfbr had a growth advantage over B10/pMC+pEDwt; in the non-selective medium, there was no significant difference in the growth rate of the two strains (Figure 1c). This result demonstrated that in strains carrying the pMC selection circuit, high L-Trp producers grew faster than low producers in medium with maltose as the sole carbon source.

Furthermore, we mixed the two strains at different initial ratios (fbr:wt = 1:9/1:3/1:1) and transferred the cultures five times. We found that the L-Trp titer/OD increased with culture transfer, regardless of the initial ratio (Figure 1d), which revealed that the high L-Trp producer was consistently enriched during transfer culture. For example, after five culture transfers, the L-Trp production increased from 4 mg/L/OD to 10 mg/L/OD in samples with an initial mixing ratio of 1:1. To confirm this enrichment effect, we subjected the mixed culture to Sanger sequencing during transfer culture. By comparing the base calling in the mix with that of the premixed sample, we estimated that during progression from G0 to G5, the ratio of high producer approximately increased from: 10% to 40% in the 1:9 mix; from 25% to 50% in the 1:3 mix; and from 50% to 70% in the 1:1 mix (Figure S4, Figure S5). Taken together, these results indicated that the pMC selection circuit enabled selection of a high L-Trp producer from a mixture of strains with different L-Trp production by simply applying the transfer culture protocol in medium with maltose as the sole carbon source.

As a control, we replaced *malQ* in the pMC circuit with *tetA* (tetracycline-resistance gene) to construct a pTet circuit, i.e., to test whether induction with varying amounts of tetracycline could also positively couple the growth rate to the intracellular L-Trp concentration in the medium (Figure S6). The selection process with the pTet circuit was initiated by adding tetracycline to the medium 3–4 h after inoculation when the OD_{600} reached 0.4–0.6 (see Methods for details). Under conditions in which the final concentration of added tetracycline was 7 mg/L, the pTet circuit in BL21(DE3) cells responded to exogenously added Ala-Trp dipeptide up to

0.6 mM (Figure S7), a plateau significantly higher than that for pMC. The increase may be caused by that the amount of L-Trp needed for sufficient expression of essential target genes for cell growth differed in a tet-containing environment. Similar to the approach we used for pMC, we constructed two strains with different L-Trp production, namely BL21(DE3)/pTet (almost no L-Trp produced) and B11/pTet (with an L-Trp titer/OD of 15 mg/L/OD). We found an optimal tet concentration (2 mg/L) to maximize the difference in their growth rates (Figure S8a). Under this condition, we obtained ~100% of the high producer after 24 h selection even when the initial ratio of the high producer in the seed solution was reduced to 10^{-4} (Figure S8b). These results demonstrated that the pTet circuit was also capable of selecting a high producer from a mixed population in the presence of inducer in the medium.

Evaluation of the Anti-escape Ability of Circuits Based on Carbon Source Utilization and Antibiotic Resistance. Before launching continuous evolution, we performed a preliminary test on the two types of circuits to compare their anti-escape properties. To investigate the escape phenomenon, we first mutated the parent strains (B1/pMC and BL21(DE3)/pTet) using biological (*dnaQ926*)[21,22] or physical (atmospheric and room temperature plasma, ARTP)[23] mutagenesis to accelerate the generation of genetic diversity (see Methods). The generated mutated strains were transferred in parallel to selective medium (M9-cas-maltose or M9-YE, with tet) or non-selective medium (M9-cas-glucose or M9-YE, without tet). We measured the OD_{600} and L-Trp titer of each culture after 24 h and transferred the evolved strains that were in the selective medium to fresh media, both selective and non-selective, and the transfer culture was repeated for several additional rounds with variable selective pressures determined according to the final OD_{600} of each individual round. Three biological replicates were included.

In these experiments, we found that L-Trp production did not increase for either parent strain (data not shown), but the growth curves differed substantially (Figure 2). By comparing the OD_{600} of strains in selective and non-selective media, we found that

for BL21(DE3)/pTet, (EGT; Figure 2) escapees arose rapidly in ≤48 h for strains mutated by *dnaQ926* (Figure 2a) and ARTP (Figure 2b), as shown by the acquisition of tet resistance without an increase in L-Trp production. The initial concentration of tet in the selective medium was set as 2 mg/L which was the optimal tet concentration for selection (Figure S8a). For strains mutated by *dnaQ926*, the stress induced by 2 mg/L tet was completely overcome when growth was measured at 72 h. At every round, we measured the rate of tet inhibition at the moment of tet addition by comparing the number of sampled bacteria that grew on agar plates with or without tet. We found decreased rates of tet inhibition for the escapees. Some escapees, which initially showed no resistance to 2 mg/L tet, acquired resistance to 4 mg/L tet just after the second round of selection; we even found escapee populations that exhibited resistance to 8 mg/L tet after the third round of selection (Figure S9). For strains mutated by ARTP, all mutated populations acquired resistance to 2 mg/L after the first round of selection and quickly adapted to 7 mg/L tet. It seemed that ARTP was more efficient at inducing gene mutations, giving rise to divergent evolutionary dynamics between the biological and physical mutators. Consequently, we used ARTP to mutate B1/pMC and repeated the same transfer culture protocol with the selective and non-selective media that we had used with *dnaQ926.* The OD_{600} measurements revealed that the evolved strains (EGM; Figure 2c) were unable to use maltose as the sole carbon source and that escapees did not appear even after 700 h, i.e., >30 rounds of selection. Taken together, the results demonstrated that, in contrast to antibiotic resistance–based systems, the novel genetic circuit based on carbon resource utilization showed an outstanding anti-escape feature, with no escapees emerging after many rounds of selection.

Previously, antibiotics were the principal agents of selection pressure. There are three major types of antibiotics,[24–26] all of which may be invalidated by adaptive mutations. For example, spontaneous resistance to tetracycline[27] of wild-type *E. coli* after adaptation was tracked to mutations that alter expression of chromosomal efflux systems[28] (such as AcrAB-TolC[29–31] and emrE[32]), modify the permeability of the outer-membrane porins or lipopolysaccharides,[33,34] or change the strength of

ribosomal binding sites.[35] Among these, intrinsic production of numerous multidrug efflux pumps bore the main responsibility for inducing broad-spectrum antibiotic resistance or substrate tolerance to poisonous substances like crystal violet, SDS, Triton X-100, etc.[36] In this context, the likelihood of generating escapees in antibiotic resistance–based selection is almost inevitable. For our novel selection system, we focused on MalQ, an enzyme that catalyzes the transglycosylation of maltose and maltodextrins in *E. coli*, an essential step in the degradation of maltose.[37,38] With a *malQ* deletion, *E. coli* cannot survive in medium with maltose as the only carbon source.[39] Therefore, the only possibility for escapees to emerge in this selection system is to acquire a chromosomal mutation in a gene that codes for an enzyme similar in function to MalQ. Based on a phylogenetic analysis of all the carbohydrate-active enzymes in *E. coli* BL21(DE3) in the Carbohydrate-Active Enzymes database[40], we found that MalQ was classified as an individual subfamily (GH77). This divergence suggested that *malQ* and the other 87 carbohydrate active enzyme–related genes have remote homologous relationships. Furthermore, if we extended to all proteins encoded by *E. coli* BL21(DE3) genome (NC_012892.2.faa), BLASTP search (*E* value = 0.01) identified no homologues to MalQ. This *in silico* analysis may explain the high anti-escape potential of this novel selection system, which is specifically based on the utilization of maltose as the sole carbon source.

In light of these considerations, we conclude that this system is potent for further application in continuous evolution to find rare beneficial mutations even at the genome level. Continuous evolution represents a powerful advance in protein engineering[41–46] and strain development[47] that may dramatically enhance the success of evolutionary approaches. Nevertheless, previous examples of continuous evolution lacked a strategy to link metabolite production to fitness, a drawback that hindered their application in metabolic engineering. Herein, we used the novel selection circuit presented here to address this issue; specifically, we performed continuous evolution to enhance L-Trp production of strains with mutations introduced both into plasmid-borne *TrpE* and genomic metabolite-processing genes.

Application of the Selection Platform to Optimize the L-Trp Biosynthetic Pathway. First, we applied the selection platform to select for a high L-Trp producer from a synthetic library. To demonstrate the selection function, we conducted site-saturation mutagenesis of the *TrpE* feedback inhibition binding site Ser40 present in the pEDwt plasmid. We transformed B10/pMC with the resulting library, named S40rd. We expected that transfer culture would allow enrichment of those bacteria that carried a mutation that released feedback inhibition; indeed, after eight cycles, the growth rate of the strains in the selective medium increased with time (Figure 3a). Furthermore, for all triplicates, the L-Trp titer/OD of the strains in the selective medium also increased over time from ~1 mg/L/OD to 10 mg/L/OD (Figure 3b). Taken together, the results showed that high L-Trp producers with high growth rates were enriched during transfer in the selective medium. As expected, the growth rate and L-Trp titer/OD remained unchanged from initial levels for transfer culture in the non-selective medium (Figure 3a and 3b). To verify the identity of the enriched mutants, we sequenced the final sample of each transfer culture at the Ser40 site. We found that three genotypes were enriched in the selective medium, namely, AGG (arginine, R), GAT (aspartic acid, D) and TTG (leucine, L) (Figure 3c). A base deletion mutation was enriched in the non-selective medium, possibly because the expression of TrpED caused burden to the cell in non-selective condition. To test the positive effect of the enriched mutations on L-Trp production, we constructed the corresponding mutant plasmids (pED-S40R/D/L) and transformed the B10 strain with each one. The L-Trp titer/OD of all mutant strains increased to levels approaching that of B10/pEDfbr (Figure 3d), which confirmed that the pMC selection circuit effectively enriched specific mutants with high L-Trp production. Previous structural analysis of TrpE revealed that the hydrogen bond formed between the amino group of L-Trp and the hydroxymethyl group on the side chain of Ser40 was responsible for feedback inhibition of anthranilate synthase by L-Trp.[48] The enriched mutant proteins bearing either arginine or aspartic acid, with their electrically charged side chain, or leucine, with a hydrophobic side chain, apparently impede the formation of the implicated hydrogen bond and thereby release feedback inhibition to ultimately

increase L-Trp titer/OD. Overall, the random nature of the selection process is supported by the fact that we did not generate Ser40Phe, a known mutant making even higher L-Trp production when cooperating with Met293Thr, and that we produced three distinct genotypes that produced high, but not the highest, production rates. Thus, the results demonstrated the potential of this approach to rapidly generate a collection of mutants with a variable range of improved production capacities.

Next, we constructed an error-prone *TrpE* library, the pED-library, to verify whether the selection circuit enriched for high producers when bacteria were transformed with a relatively large and undefined mutational library. We transformed B10/pMC with the pED-library and applied transfer culture. We performed six replicates for transfer culture in the selective medium; only a single sample was cultured in the non-selective medium because of the inherent randomness of the selection. The cultures were viable for 20 transfers. In the selective medium, the samples from the sixth replicate exhibited a significant increase in both L-Trp titer/OD (Figure 4a) and growth rate (Figure S10), whereas in the non-selective medium, the L-Trp titer/OD remained essentially unchanged. From generations 12 and 16 (G12 and G16), we isolated 24 single colonies from the culture of replicate No. 6 in the selective medium (lib-M6 at G12 and G16) and 12 single colonies from culture in the non-selective medium (lib-G at G12 and G16). We chose generation 12 for its highest L-Trp titer/OD among the total 20 generations and thus we anticipated that the possibility of isolating best mutants is higher. As the titer/OD of generation 13, 14 and 16 are the second highest and are almost the same, we chose generation 16 as it is 4 generations away from generation 12 and we anticipated that more genetic changes would be found from generation 16 other than generation 13 and 14 as they are closer to generation 12. We sequenced the *TrpE* region on the corresponding plasmids. The sequencing results are shown in Table 1. Two mutants, mutant1 (V68I, V228A, H459Q) and mutant2 (A156T) were enriched in the selective medium, and the fraction of mutant1 increased from 70% to 100% from G12 to G16. In the non-selective medium, only one mutant, mutantC (P273H, A327V), was enriched in both G12 and G16. We then constructed three plasmids, each one harboring one of the

different enriched mutations, called pED-mutant1, pED-mutant2, and pED-mutantC. We used them to transform B10/pMC and different B10 pED-carrying strains and measured the corresponding L-Trp production in M9-cas-glucose medium. Both B10/pMC and B10 pED-mutant strains (-mutant1 and -mutant2) exhibited an ~two-fold increase in L-Trp production compared with B10 pEDwt that carried the parental plasmid; the productivity of pED-mutantC was similar to that of pEDwt (Figure 4b). The mutations identified in mutant1 and mutant2 were not known to increase L-Trp production; thus, we concluded that the selection method permitted discovery of novel beneficial mutations from within a relatively large and undefined mutational library. The fact that mutant1 finally overtook the population may be due to some other unknown beneficial mutations in the genome causing different dynamics of L-Trp production or different distribution of the subpopulation caused by non-genetic variation within isogenic populations[49], some possibilities to be further investigated. And from the perspective of enzyme structure, future work may focus on precisely how the mutations in *TrpE* (V68I, V228A, H459Q, A156T) discovered in this study contribute to the observed increase in L-Trp production.

Taken together, these results indicate that this new approach is a powerful and flexible tool for high-throughput engineering of proteins. In a validated selection system for targeted protein function, it quickly identifies novel active sites, even as encoded by vast mutant libraries.

Application of the Selection Platform for Mutational Breeding of L-Trp High Producers at the Level of the Genome. Although our knowledge about microbial metabolism is increasing with the detailed functional annotation of each gene, research[50] suggests that genes currently without direct links to target metabolite networks may have an unexpected impact on the future choice and elaboration of microbial cell factories. For this reason, we tested our strategy on the evolutionary engineering of high L-Trp producers through random mutagenesis of the whole genome followed by targeted selection. It is likely that genome-wide mutations beneficial to metabolite production are much less frequent than neutral or cheater

mutations. Only by reducing the escape rate—as in the present strategy—can we establish effective selection filters for desired traits. Naturally occurring mutations in most microbes are rare and thus, they are far from satisfying the demanding requirements of engineering applications. Accordingly, our experiments began with ARTP mutagenesis to accelerate the generation of genetic diversity. From the results of our previous preliminary test, we had found that even though our platform was very robust, we could not obtain the high L-Trp producer phenotype from a B1/pMC strain with a comparatively wild-type genotype, even after >700 h of transfer selection. As L-Trp biosynthesis is related to several metabolic pathways, acquisition of the high Trp-producer phenotype would likely require the simultaneous alteration of multiple genes. To expedite the generation of new beneficial mutations at the genome level, we constructed a strain, B12, in which we modified all the known critical sites related to L-Trp biosynthesis. B12 mutational changes included removing competitive pathways, blocking downstream L-Trp degradation pathways, and enhancing synthetic routes. We used B12 to construct a new parental strain carrying the pMC2 plasmid, which was derived from pMC by adding the constitutively expressed *sacB* gene to help counter-selection when we want to eliminate the plasmids from host cells. B12/pMC2 was mutated by ARTP and subjected to continuous evolution. The L-Trp production of evolved populations in selective media changed over time (Figure 5a), and, after increasing in early rounds, it remained relatively stable up to at least G15. We randomly selected 15 single colonies from G4, G11, and G14 of each parallel experiment to assess L-Trp production in the non-selective medium. We chose G11 as its L-Trp production in three parallel experiments was all in relatively high levels for the first time. And G4 and G14 were chosen to help us learn more about the evolutionary trace of our selection. The incremental rate of L-Trp production of the picked strains was plotted against that of the parental strain, and the results showed different evolutionary trajectories (Figure S11). Finally, we selected several of the highest producing strains to confirm their production. The results showed that we had obtained strains with production levels increased by ~55–65%; in several instances, this was achieved after only a few rounds

of selection (G1–G4; Figure 5b). To make sure the increase of L-Trp production was caused by mutations on the genome, we further extracted the pMC2 plasmids from the evolved strains shown in Figure 5b and retransformed the original pMC2 plasmids into them. The production of new strains remained the same with the picked evolved ones and was higher than the parent strains (data not shown). This result indicated that it was the mutations on the genome that contributed to the phenotype. Then, we performed the genome sequencing on five evolved strains (EGMB81-G11-1/pMC, EGMB81-G14-2/pMC, EGMB82-G4-1/pMC, EGMB83-G11-2/pMC, EGMB83-G14-1/pMC) and summed up the mutation sites in the genome scale map of parent strain (Figure S12). Some sites (*pcnB*, *rihC*) were related to DNA replication and repair, while others were mainly concerned with metabolic reactions. Further detection need to be done to figure out the effective sites. Collectively, these existing results amply demonstrated the efficacy of this selection method in the discovery of rare and beneficial novel mutations at the genome level, which constitutes an important advance in strain development both for industrial production and in-depth mechanistic studies.

From all the experiment above, we found that several crucial issues required further discussions in our strategy. First, the operational range of a selection circuit, defined as the chemical concentration range in which microbes continue to experience growth advantage as the concentration increases,[14] determines the utility of the selection circuit for improving metabolite production, so it should be tuned seriously. The upper boundary of the operational range defines the limit that production optimization can reach. Here, the upper boundary of the pMC circuit was 20 μM Ala-Trp(exogenously added). To increase the upper limit of the pMC circuit and thereby extend its utility for pathway optimization, there were two possible strategies: adding a degradation-encoding tag to *malQ* to accelerate MalQ proteolysis or reducing the ribosomal binding site strength of the *malQ* mRNA to attenuate translation. Furthermore, for the selection to be sufficiently strict, the basal expression of *malQ* must be lowered. As the sensor itself primarily determines basal expression,

and because most natural sensors may not have evolved to completely repress the basal expression of the genes they control, a promising approach may be to reduce basal expression through sensor mutation followed by selection for a stricter sensor. Second, although we picked out strains with increased production in both experimental approaches finally, we still found that the L-Trp titer/OD first rose and then, in some cases, declined. We surmise that as the titer/OD increases, the stress may become progressively less strict and consequently lead to a greater possibility that irrelevant mutations may predominate in the population. As this risk would be expected to increase with time as spontaneous mutations accumulate, the number of selection cycles should be limited to a reasonable time range. Third, it should be admitted that the increase in L-Trp production of evolved strains was not very remarkable in our work. It might be blamed on the impossibility of generating strains with multiple beneficial mutations in the limited selection time, so the mutation sites we found were supposed to be locally optimal solutions. Our results indicated that we can easily find non-intuitive and specific mutations in different parallel experimental groups. By combination of these mutations, there is a hope for further improvement of production. And looking at it from another point of view, our selection systems can serve as a powerful discovery platform to provide abundant raw research materials for deep learning in biological mechanism study.

In summary, we believe that the strategy of the novel selection circuit defined in this work shows much potential for providing a framework for improving directed synthesis of other trait-oriented chemicals by microbial cell factories.

METHODS

Strains and Culture Conditions. Strains and plasmids are described in Table 2. The red recombination method[51] was used for gene knockout. The following standard culture protocols were used throughout: to generate seed cultures, single colonies

from plates were inoculated into 5 mL LB medium in 15-mL centrifuge tubes (BD) and cultured overnight at 37ºC at 200 rpm. Experimental cultures were started from seed cultures by inoculation into 10 mL medium in a 50-mL flask to an initial OD_{600} of 0.02 and incubated as above for 24 h or the times indicated. For growth to log phase, OD_{600} was monitored throughout culturing.

Media. M9-cas-maltose medium: 4 g/L maltose, M9 salts (17.1 g/L $Na_2HPO_4•12H_2O$, 3 g/L KH_2PO_4, 0.5 g/L NaCl, 1 g/L NH_4Cl), 2 mM $MgSO_4$, and 0.1 mM $CaCl_2$, 1g/L casamino acids (J851, Amresco, Solon, OH),[52] 0.34g/L thiamine pyrophosphate (Sigma-Aldrich, cat. no. C8754-1G). M9-cas-glucose medium: 4 g/L glucose, M9 salts, 2 mM $MgSO_4$, and 0.1 mM $CaCl_2$, 1g/L casamino acids,[52] 0.34g/L thiamine pyrophosphate. M9-YE medium: 5 g/L glucose, M9 salts, 1 g/L yeast extract, 1 mM $MgSO_4$, and 0.1 mM $CaCl_2$. As appropriate, addition of 100 mg/L ampicillin, or 34 mg/L or 14 mg/L chloromycetin to the media was used to maintain the presence of corresponding drug-resistant plasmids.

Plasmid Construction. All the oligonucleotides used in this work were purchased from Taihe Biotechnology Co., LTD (Beijing, China) and listed in Table S1. Construction of individual plasmids is described below.

Construction of pMC, pTet, and pMC2. The pMC plasmid contains *malQ*, PCR-amplified from the *E. coli* BL21(DE3) genome using the primer of pTrc99a-MalQ-F/pTrc99a-MalQ-R and fused downstream to the *tnaC* regulatory element of the tnaCAB operon, PCR-amplified from pSenTrp using the primer of tnaC-tnaA-UP-F/tnaC-tnaA-UP-R.[53] The *trc* promoter of pTrc99A was substituted with the pBAD promoter (PCR-amplified from pNotgate) along with the *araC* regulatory element of the ara operon upstream of the pBAD promoter by Gibson assembly.[54] The PCR-amplified fragments of *malQ* and the *tnaC* regulatory element were ligated into the multiple cloning site of the modified pTrc99A plasmid by Gibson assembly to construct pMC. *tnaC* acts as the L-Trp sensor[55] to transform the

signal of the intracellular L-Trp concentration into the expression of the downstream *malQ*. pTet was constructed by replacing *malQ* in pMC with *tetA* and adding *dnaQ926* controlled by the pBAD promoter. pMC2 was built by adding the constitutively expressed *sacB* to pMC upstream of *Amp*.

Construction of pEDwt and pEDfbr. Plasmid pEDfbr was constructed by substituting the T7 promoter of pEDori with the J23109 promoter from the Registry of Standard Biological Parts (partsregistry.org) and by substituting the p15A origin of replication of pEDori with that of pSC101 (PCR-amplified from pNotgate). pEDwt was constructed by introducing two point mutations into *TrpE*: Phe40Ser (TTC to TCC), and Thr293Met (ACG to ATG).

Construction of the Plasmid Library of pED-S40SSM. Plasmid pEDwt was PCR-amplified by two pairs of primers S40rd-F/Inner-R and Inner-F/S40rd-R, and the two amplified fragments were ligated by Gibson assembly to form the site-saturation mutagenesis library of the *TrpE* S40 site. The S40rd-F primer contains NNK to cover the TCC codon of the S40 *TrpE* site. The sequence of S40rd-F primer is: 5′-TCGTCCGGCAACGCTGCTGCTGGAANNKGCAGATATCGACAGCAAAGATG-3′.

Preparation of the Error-prone *TrpE* Library, pED-Library. The *TrpE* fragment was amplified with error-prone PCR using the primer pair of PF_TrpE_eplib/PR_TrpE_eplib from pEDwt to form the fragment TrpE-ep. Then the backbone fragment of pEDwt was amplified by the primer pair of PF_pEDbackbone/PR_pEDbackbone and was ligated with the TrpE-ep fragment by Gibson assembly to form the *pED-library*. The concentration of Mn^{2+} used in the error-prone PCR protocol was 0.1 mM, and the corresponding mutation rate was ~3.5 nucleotides/molecule measured by calculating the mean mutation rate of 10 randomly selected colonies.

Characterization of pMC. For the characterization of the pMC circuit with exogenously added Ala-Trp, we used the B1/pMC strain in M9-cas maltose medium with 0.1 g/L L-arabinose, and cultures were grown to log phase. To compare the growth rate of strains with different L-Trp productivities, we used the strains B10/pMC+pEDwt and B10/pMC+pEDfbr grown to log phase in M9-cas maltose medium.

Growth Selection for pMC. For the growth selection of the mutagenic library, the library plasmids (site-saturation mutagenesis library, pED-S40SSM, or error-prone PCR library, pED-library) were transformed individually by electroporation into strain B10/pMC. Ten times the number of library size transformants were scraped off the plate and inoculated both into selective medium (M9-cas-maltose medium with 3.8 g/L maltose and 0.2 g/L glucose) and non-selective medium (M9-cas-glucose medium). For the transfer cultures, when the OD_{600} of strains in the selective medium reached 0.8–1.0, the cultures were transferred into fresh medium and denoted as generation n+1.

Generation of Mutational Library by *dnaQ926*. Parent strains, after culture in LB medium for 16 h, were transferred to fresh LB medium (1:100, v:v) with 1 g/L L-arabinose to induce expression of *dnaQ926*, which increased the mutation rate by 10-fold compared with the natural mutation rate (data not shown). Strains were cultured in this medium for another 24 h and used as the initial mutational library.

Generation of Mutational Library by ARTP. Parent strains, after culture in LB medium for 16 h, were transferred to fresh LB medium (1:100, v:v). When OD_{600} reached ~ 0.8, 10 μL culture solution was spread on a sterile iron plate to be irradiated by ARTP for 25 s with a power of 100 W and a gas flow of 10 SLM. Strains were washed from the plate and culture resumed in the non-selective medium for 24 h to generate the initial mutational library.

Characterization and Evolution Process for the pTet Circuit. For the pTet circuit, selection was performed by adding tet to M9-YE medium (non-selective) when the OD_{600} of strains reached 0.4–0.6. Growth was monitored for 20 h to see how the circuit responded to exogenously added Ala-Trp or to L-Trp producers with different production capacities. For continuous evolution, cultures were transferred every 24 h and tet was added as above for every round of selection. OD_{600} and L-Trp production were tested at the end of each selection, and 500 μL of the evolved strain was stocked in 50% glycerol solution at –20ºC.

Quantification of Extracellular L-Trp and Maltose. The extracellular L-Trp titer was measured for each generation after 24 h of fermentation starting from single-colony preparations. For the quantification of L-Trp, culture samples were centrifuged at 18,000 ×*g* for 10 min, and 500 μL of each supernatant was separated in an Inertsil ODS-SP 4.6 × 250 mm column using a Shimadzu HPLC system. The mobile phase was methanol (A) and 0.05% (w/v) aqueous H_3PO_4, and the UV detector was set to 280 nm. The elution procedure was 2% A between 0–3 min; 2–80% A between 3–30 min; 80% A between 30–40 min; 80–2% A between 40–50 min; and 2% A between 50–60 min with a flow rate of 0.5 mL/min. For the detection of maltose, culture samples were prepared as above, and 500 μL of each supernatant fraction was separated in an Aminex HPX-87H, 300 × 7.8 mm column using the Shimadzu HPLC system. The mobile phase was 5 mM aqueous H_2SO_4 with a constant flow rate of 0.8 mL/min, and it was analyzed with a refractive index detector (RID-10A, Shimadzu).

Figure and Table legends

Figure 1. pMC circuit in genomic malQ knockout environment: L-Trp–dependent glucose production. (a) Mechanisms of the pMC selection circuit in the growth-production coupling function and the selection process to enrich for high producers from a library of mutants with different L-Trp production. (b) Growth response of the pMC circuit towards exogenously added Ala-Trp. Fitness plateaued at Ala-Trp >20 μM. NC: strains without pMC circuit. Data represent the mean ± SD; n = 3. (c) Growth curves for B10/pMC: +pEDwt or +pEDfbr, in selective or non-selective medium. (d) L-Trp titer/OD of the mixed cultures during transfer culture. Gx: generation x, where x = 1, 2, 3, 4, or 5, i.e., the number of culture transfers. Mix 1:9, 1:3, or 1:1 indicates the initial ratio of B10/pMC+pEDwt to B10/pMC+pEDfbr. Data in Figure 1b and 1c represent the mean ± SD; n = 3.

Figure 2. Evaluation of anti-escape ability of circuits based on carbon source utilization and on antibiotic resistance. (a) The growth curve for each evolved strain population from BL21(DE3)/pTet, mutated by *dnaQ 926*, in selective and non-selective media. Arrows show times of tet addition. (b, c) Growth curves in selective or non-selective medium for each evolved strain population from (b) BL21(DE3)/pTet, mutated by ARTP, to give EGT strains 1–3, and from (c) B1/pMC, mutated by ARTP, to give EGM strains 1–3. Three biological parallel studies were done in each experiment.

Figure 3. Application of the selection method to a site-saturation mutagenesis library targeting the S40 feedback inhibition binding site of TrpE. (a) Growth curve for strains during transfer culture. S40rd-1, -2, and -3 denote triplicate samples from the S40rd mutagenesis library in the selective medium, and S40rd-C denotes a sample of the same library cycled in non-selective medium. (b) L-Trp titer/OD during culture transfer for G1–G8. After 24 h of culture, the extracellular titer/OD of L-Trp was measured. (c) Base calling of the TrpE S40 site at G1 and G8. Nucleotide bases: green, A; black, G; blue, C; red, T. Three genotypes (AGG, GAT, TTG) were enriched in selective medium, and one genotype (AC with one base deletion) was enriched in non-selective medium. (d) L-Trp titer/OD of the three enriched mutants pED-S40R, pED-S40D, and pED-S40L. Single-site mutagenesis was conducted to produce the corresponding mutations on pEDwt. Strain B10 was transformed with each of the plasmids, and L-Trp production was measured after 24 h of fermentation. Data in Figure 3d represent the mean ± SD; n = 3.

Figure 4. Application of the selection method to the error-prone TrpE library. (a) Extracellular titer/OD of L-Trp measured after 24 h of transfer culture. lib-M1–6: Six replicates from selective medium; lib-G: single sample from non-selective medium. (b) L-Trp titer/OD of three reconstructed strains. Site mutagenesis of pEDwt generated three plasmids, each carrying one of the mutations found in the enriched mutants. B10/pMC and B10 were each transformed with the individual plasmids, and

L-Trp production was measured after 24 h of fermentation. Data in Figure 4b represent the mean ± SD; n = 3.

Figure 5. Application at the genome level of the selection platform for mutational breeding of L-Trp high producers. (a) L-Trp production of three high L-Trp producers, i.e., the evolved B12/pMC2 strains EGMB81, EGMB82 and EGMB83, monitored over 20 selection cycles. Three biological parallel studies were done. (b) Production as measured at several selected generations of the high L-Trp producers in (a). Data in Figure 5b represent the mean ± SD; n = 3.

Table 1 Percent enriched mutants in G12 and G16

Table 2 List of strains and plasmids

Figures:

Fig. 1a)

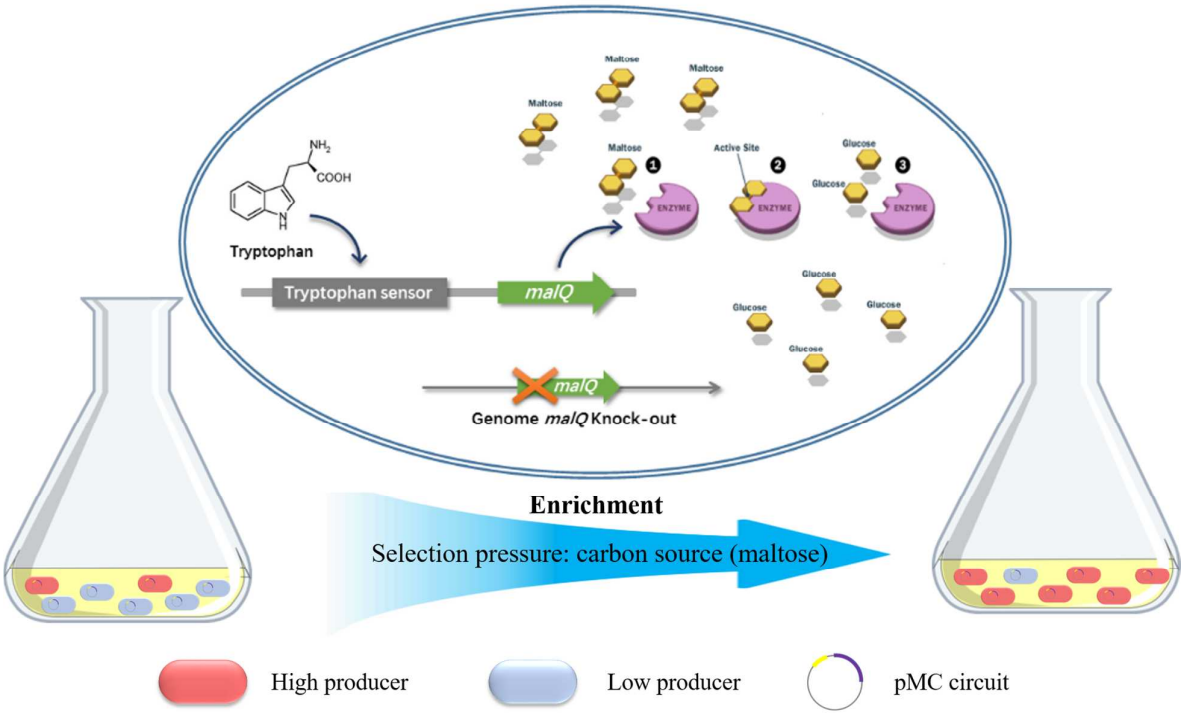

Fig. 1b)

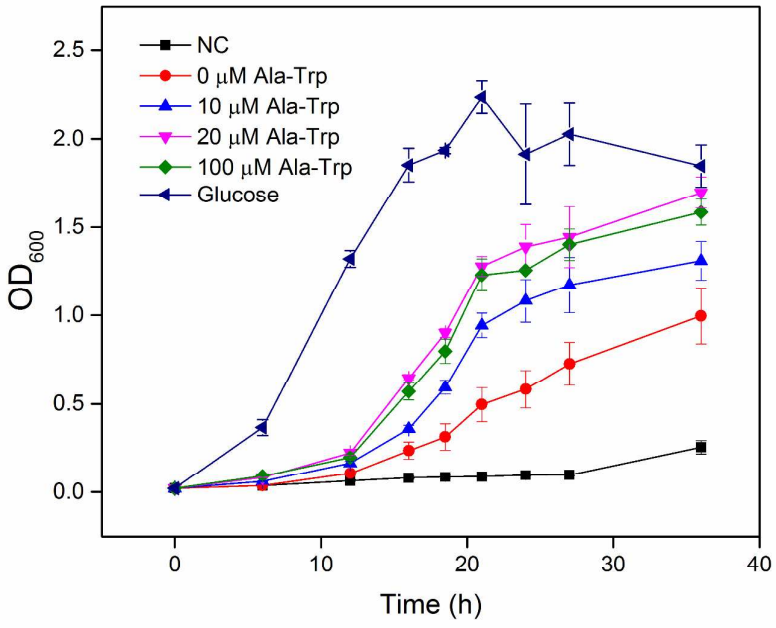

Fig. 1c)

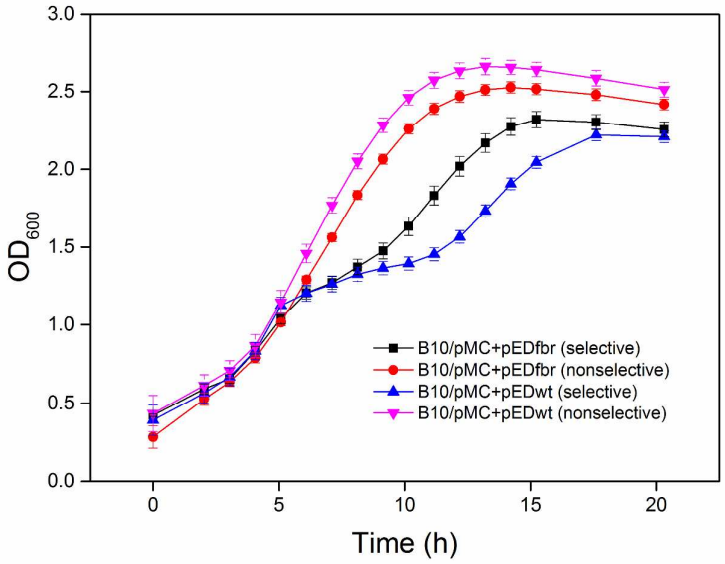

Fig. 1d)

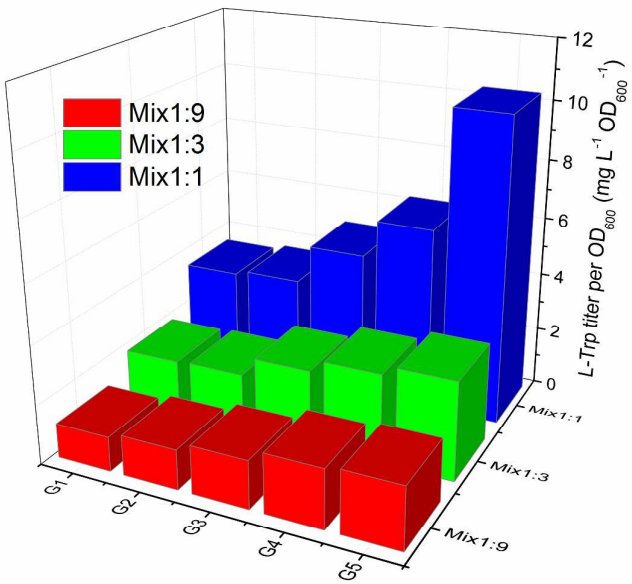

Figure 1. pMC circuit in genomic malQ knockout environment: L-Trp–dependent glucose production. (a) Mechanisms of the pMC selection circuit in the growth-production coupling function and the selection process to enrich for high producers from a library of mutants with different L-Trp production. (b) Growth response of the pMC circuit towards exogenously added Ala-Trp. Fitness plateaued at Ala-Trp >20 µM. NC: strains without pMC circuit. Data represent the mean ± SD; n = 3. (c) Growth curves for B10/pMC: +pEDwt or +pEDfbr, in selective or non-selective

medium. (d) L-Trp titer/OD of the mixed cultures during transfer culture. Gx: generation x, where x = 1, 2, 3, 4, or 5, i.e., the number of culture transfers. Mix 1:9, 1:3, or 1:1 indicates the initial ratio of B10/pMC+pEDwt to B10/pMC+pEDfbr. Data in Figure 1b and 1c represent the mean ± SD; n = 3.

688 Fig. 2a)

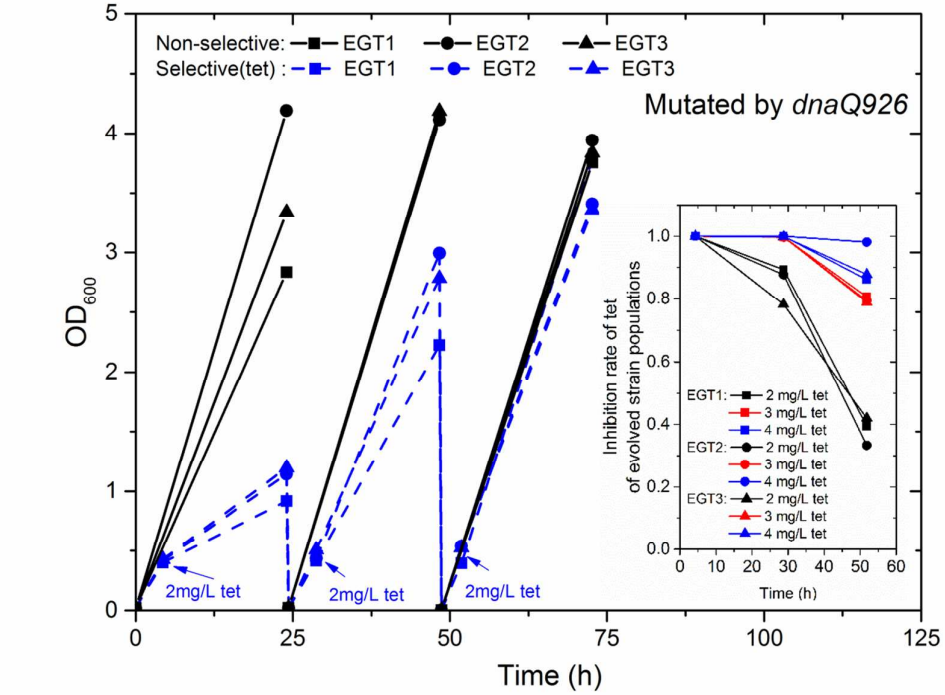

689 Fig. 2b)

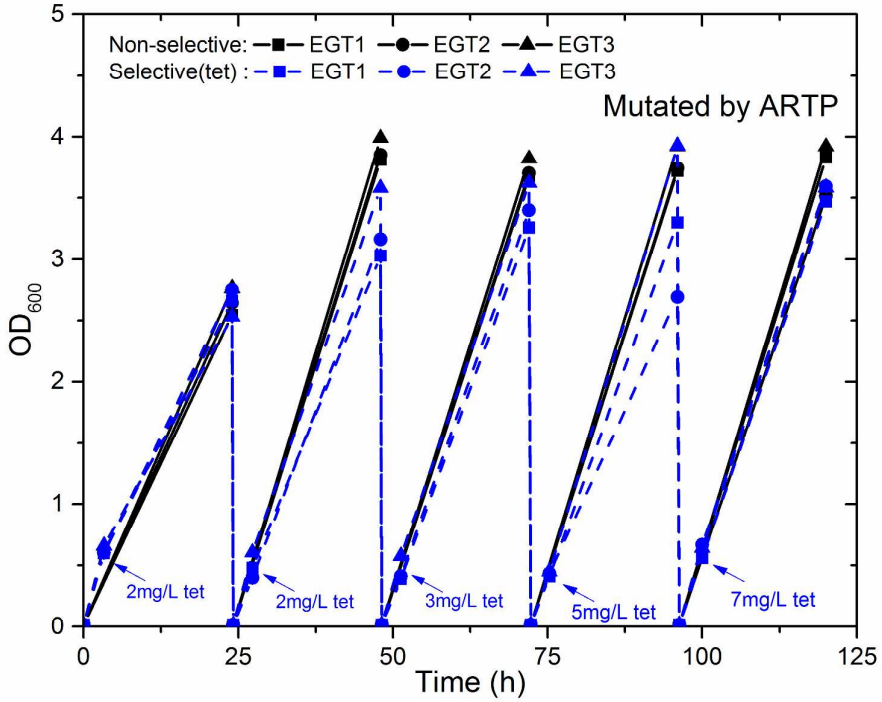

690

691

692

693

Fig. 2c)

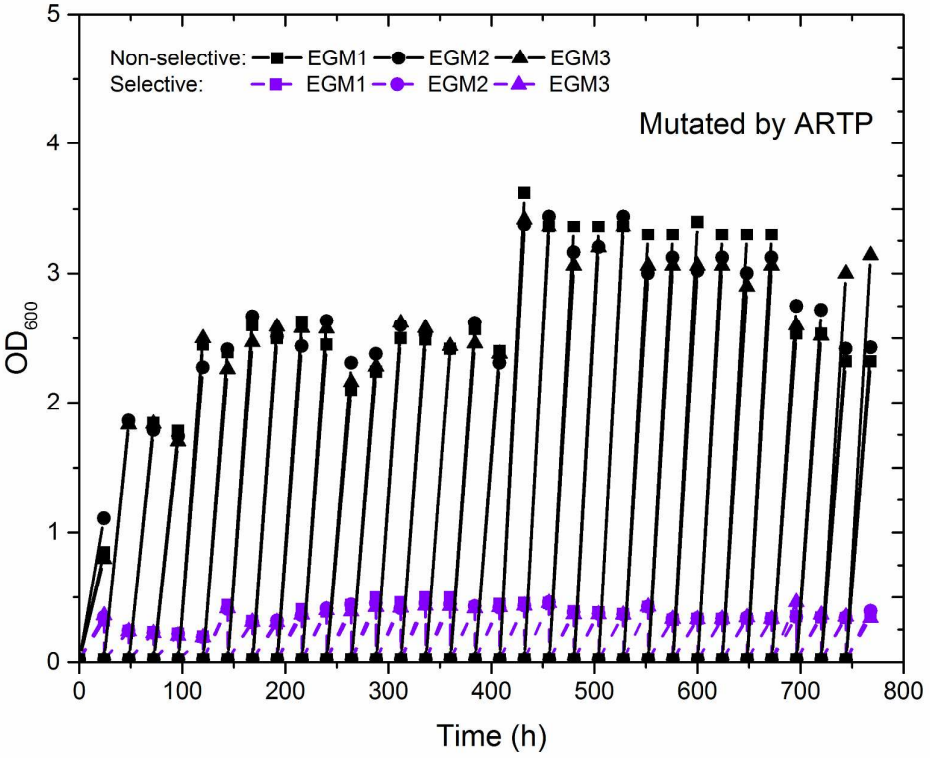

Figure 2. Evaluation of anti-escape ability of circuits based on carbon source utilization and on antibiotic resistance. (a) The growth curve for each evolved strain population from BL21(DE3)/pTet, mutated by dnaQ 926, in selective and non-selective media. Arrows show times of tet addition. (b, c) Growth curves in selective or non-selective medium for each evolved strain population from (b) BL21(DE3)/pTet, mutated by ARTP, to give EGT strains 1–3, and from (c) B1/pMC, mutated by ARTP, to give EGM strains 1–3. Three biological parallel studies were done in each experiment.

706 Fig. 3a)

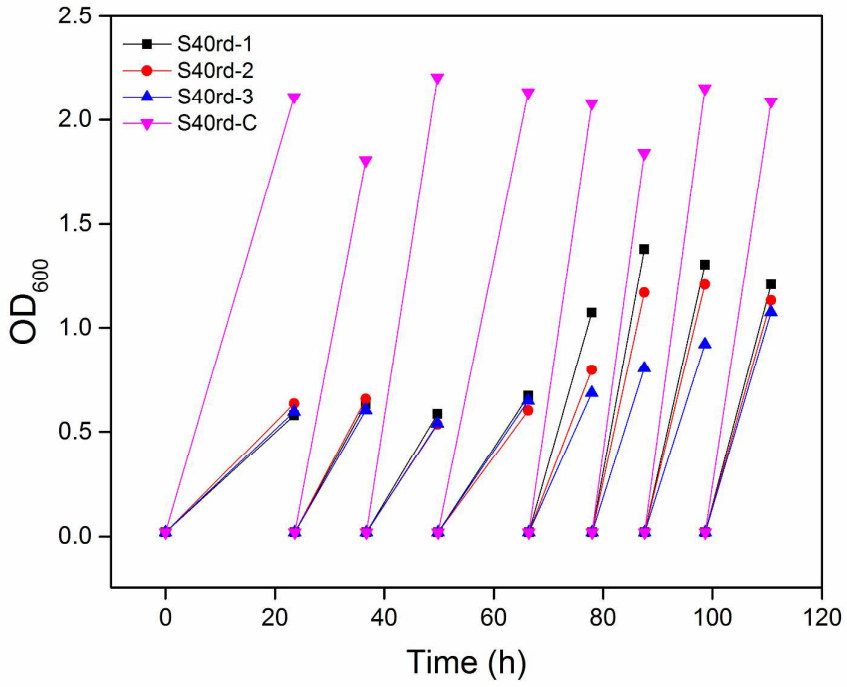

707

708 Fig. 3b)

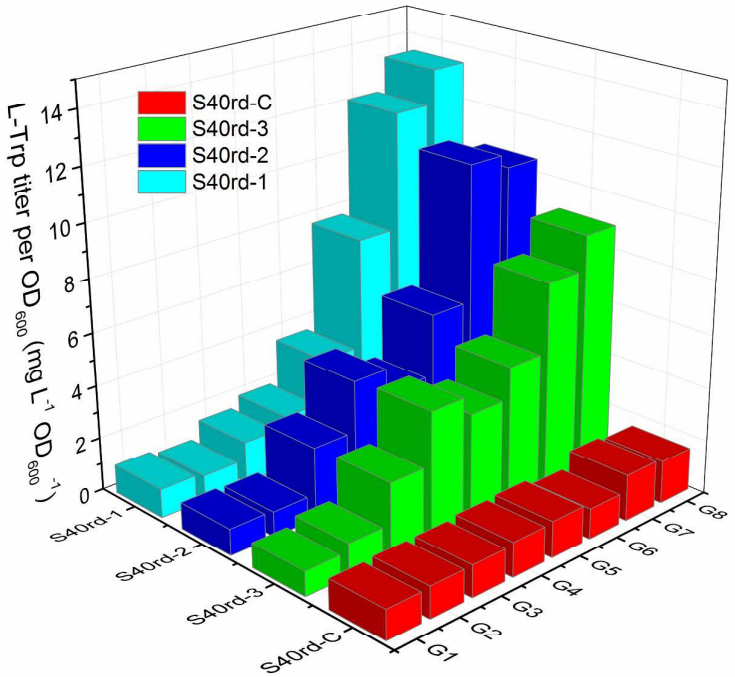

709

Fig. 3c)

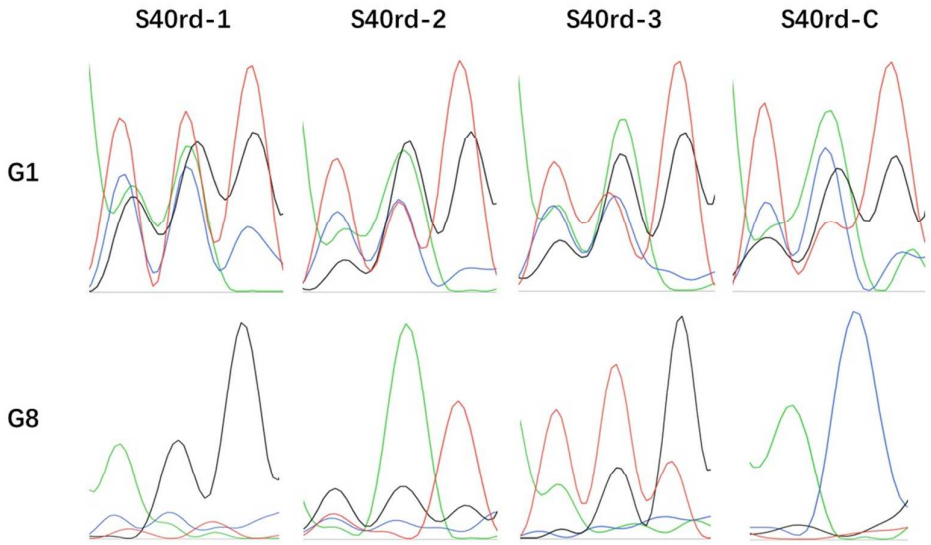

Fig. 3d)

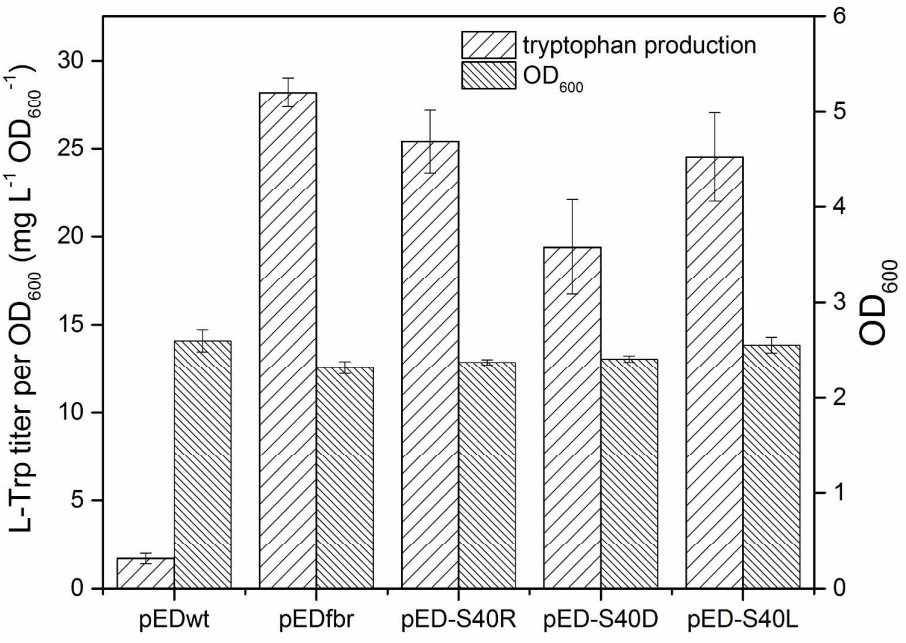

Figure 3. Application of the selection method to a site-saturation mutagenesis library targeting the S40 feedback inhibition binding site of TrpE. (a) Growth curve for strains during transfer culture. S40rd-1, -2, and -3 denote triplicate samples from the S40rd mutagenesis library in the selective medium, and S40rd-C denotes a sample of the same library cycled in non-selective medium. (b) L-Trp titer/OD during culture transfer for G1–G8. After 24 h of culture, the extracellular titer/OD of L-Trp was

measured. (c) Base calling of the TrpE S40 site at G1 and G8. Nucleotide bases: green, A; black, G; blue, C; red, T. Three genotypes (AGG, GAT, TTG) were enriched in selective medium, and one genotype (AC with one base deletion) was enriched in non-selective medium. (d) L-Trp titer/OD of the three enriched mutants pED-S40R, pED-S40D, and pED-S40L. Single-site mutagenesis was conducted to produce the corresponding mutations on pEDwt. Strain B10 was transformed with each of the plasmids, and L-Trp production was measured after 24 h of fermentation. Data in Figure 3d represent the mean ± SD; n = 3.

Fig. 4a)

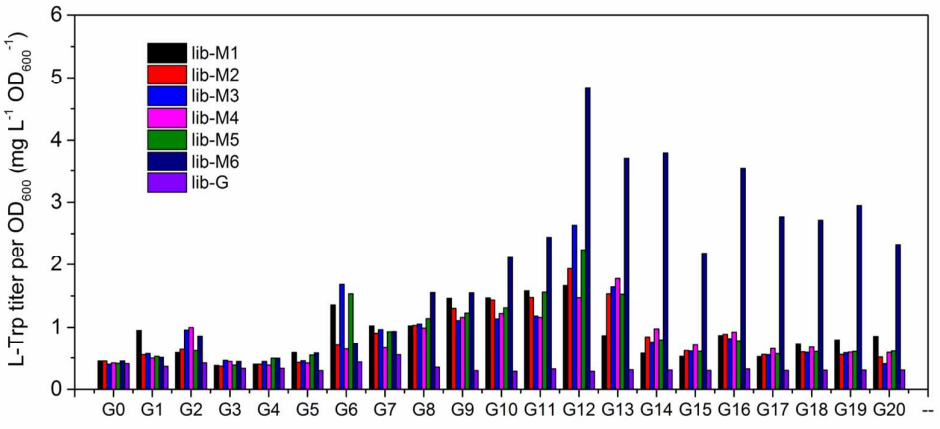

Fig. 4b)

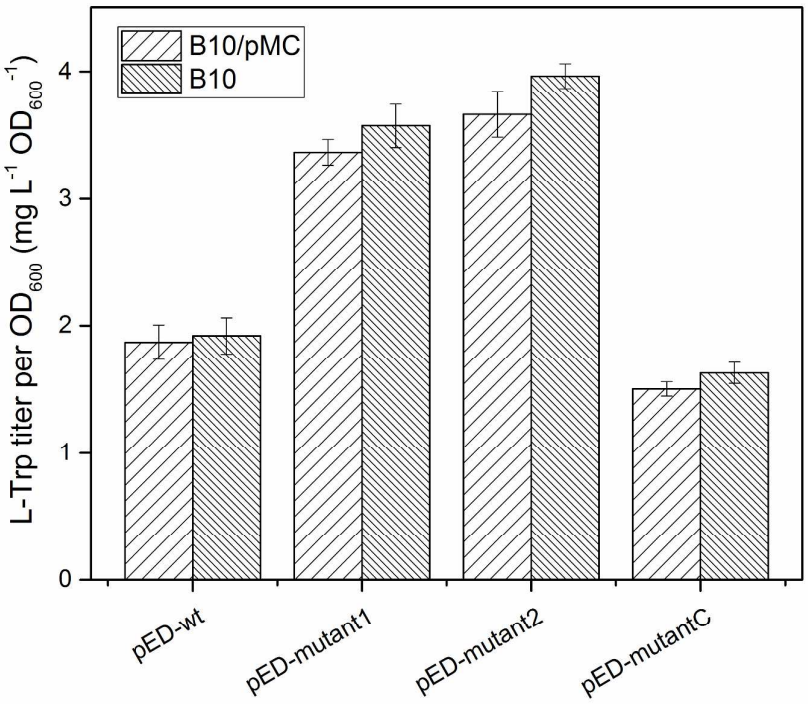

Figure 4. Application of the selection method to the error-prone TrpE library. (a) Extracellular titer/OD of L-Trp measured after 24 h of transfer culture. lib-M1–6: Six replicates from selective medium; lib-G: single sample from non-selective medium. (b) L-Trp titer/OD of three reconstructed strains. Site mutagenesis of pEDwt generated three plasmids, each carrying one of the mutations found in the enriched mutants. B10/pMC and B10 were each transformed with the individual plasmids, and L-Trp production was measured after 24 h of fermentation. Data in Figure 4b represent the mean ± SD; n = 3.

Fig. 5a)

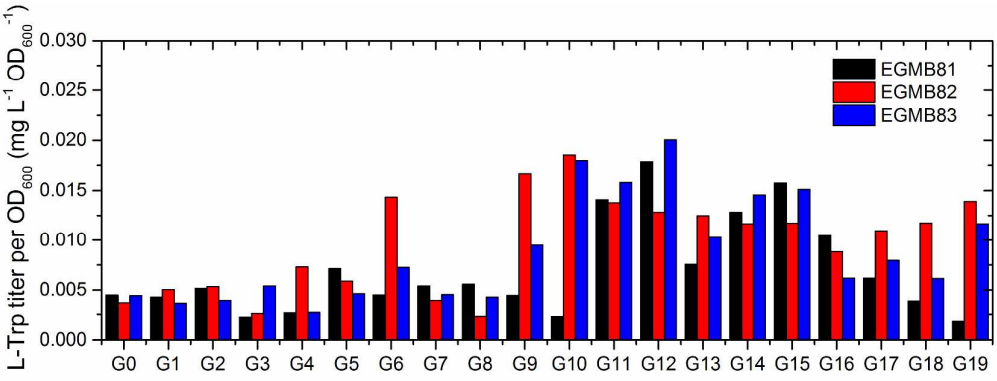

Fig. 5b)

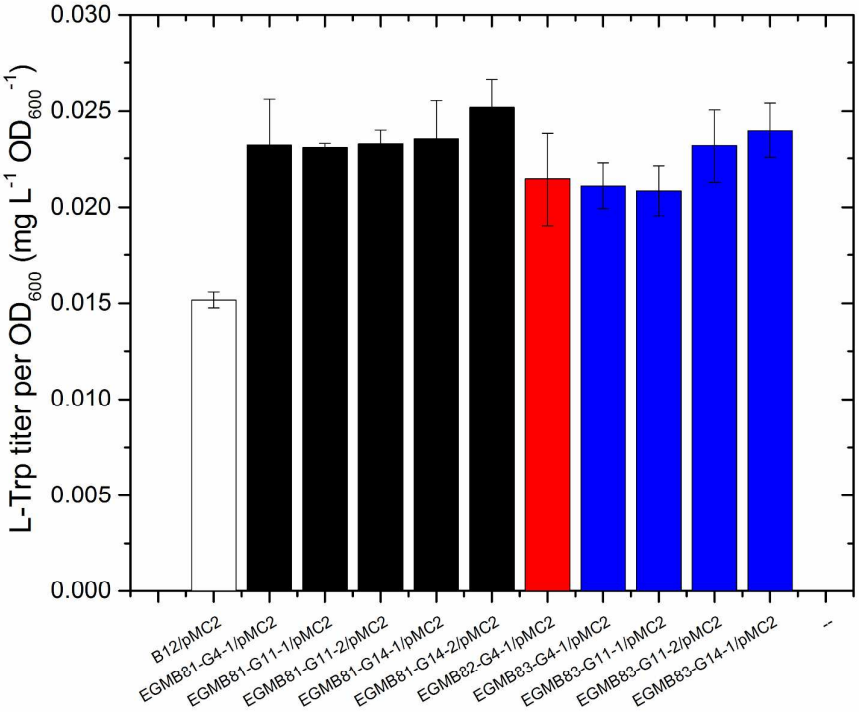

Figure 5. Application at the genome level of the selection platform for mutational breeding of L-Trp high producers. (a) L-Trp production of three high L-Trp producers, i.e., the evolved B12/pMC2 strains EGMB81, EGMB82 and EGMB83, monitored over 20 selection cycles. Three biological parallel studies were done. (b) Production as measured at several selected generations of the high L-Trp producers in (a). Data in Figure 5b represent the mean ± SD; n = 3.

Tables:

Table 1. Percent enriched mutants in G12 and G16

	Mutant	G12	G16
Selective medium	1	69.6%	100%
	2	30.4%	0%
Non-selective medium	C	100%	100%

Table 2. List of strains and plasmids.

Bacterial strains or plasmids	Characteristics	Source
Strains		
BL21(DE3)	Wild-type	Fang[a]
B1	*E. coli* BL21(DE3) *ΔmalQ ΔaraA*	This study
B8	*E. coli* BL21(DE3) *ΔTrpR ΔtnaA ΔpheA*	Fang[a]
B10	B8 *ΔaraA ΔmalQ*	This study
B11	B8 *ΔTrpED ΔaraA::(CmR^R) ΔxylA::(M1-46-TrpE^{fbr}D)*	This study
B12	B11 *ΔmalQ*	This study
Plasmids		
pTrc99A	pBR332 origin, *trc* promoter, *Amp^R*	Novagen
pSenTrp	pTrc99A with regulatory element of tnaCAB operon and *egfp, Amp^R*	Fang[a]
pNotgate	pBAD promoter, *araC* regulatory element of ara operon, *Amp^R*	Provided by Lou[b]
pMC	pSenTrp with *malQ* downstream; the regulatory element of tnaCAB operon controlled by pBAD promoter, *araC*, *Amp^R*	This study
pTet	pSenTrp with *tetA* downstream the regulatory element of tnaCAB operon controlled by p$_{rha}$BAD promoter, *araC*, *Amp^R*, *dnaQ926* controlled by pBAD promoter	This study
pMC2	pMC with *sacB* constitutively expressed to help circuits lose	This study
pEDori	pACYCDuet with *TrpE^{fbr}D* (Ser40Phe TCC to TTC; Met293Thr ATG to ACG), *CmR^R*	Fang[a]
pEDwt	pACYCDuet with *TrpED*, J23109 promoter, pSC101 origin, *Cm^R*	This study
pEDfbr	pACYCDuet with *TrpE^{fbr}D*, J23109 promoter, pSC101 origin, *Cm^R*	This study
pED-S40SSM	pEDwt with Ser40 site-saturated mutagenesis	This study
pED-S40R	pEDwt with Ser40Arg TCC to AGG	This study
pED-S40D	pEDwt with Ser40Asp TCC to GAT	This study
pED-S40L	pEDwt with Ser40Leu TCC to TTG	This study
pED-library	pEDwt with *TrpE* library generated by error-prone PCR, *Cm^R*	This study
pED-mutant1	pEDwt with V68I, V228A and H459Q	This study
pED-mutant2	pEDwt with A156T	This study
pED-mutantC	pEDwt with P273H / A327V	This study

[a]17. [b]56.

Supporting Information

Figures: fluorescence-based response data of L-Trp biosensors; response curves of pMC circuit based on maltose consumption; L-Trp production and growth of B10/pEDwt and B10/pEDfbr; base calling of the premix culture of the S40 site of TrpE; base calling of the S40 site of TrpE at generations 0, 3 and 5; mechanism of pTet circuit; response curves of the pTet circuit; effect of the pTet circuit on enrichment of high producers; characterization of an escapee from BL21(DE3)/pTet; growth rates during transfer culture of strains with the error-prone TrpE library; incremental rates of L-Trp production of the picked evolved strains with mutations at genomic level; list of mutation sites. Tables: oligonucleotides used in this work.

AUTHOR INFORMATION

Corresponding Authors

[*]**E-mail:** chongzhang@tsinghua.edu.cn

Author Contributions

[2]These authors contributed equally to the work

Notes

The authors declare no competing financial interest.

ACKNOWLEDGMENTS

This work is supported by National Key Scientific Instrument and Equipment Project of NSFC (2162780028) and the Tsinghua University Initiative Scientific Research Program (20161080108).

REFERENCES

(1) Dragosits, M., and Mattanovich, D. (2013) Adaptive laboratory evolution - principles and applications for biotechnology. *Microb. Cell Fact. 12*, 64.

(2) Portnoy, V. A., Bezdan, D., and Zengler, K. (2011) Adaptive laboratory evolution-harnessing the power of biology for metabolic engineering. *Curr. Opin. Biotechnol. 22*, 590–594.

(3) Wisselink, H. W., Toirkens, M. J., Berriel, M. D. R. F., Winkler, A. A., Van Dijken, J. P., Pronk, J. T., and Van Maris, A. J. A. (2007) Engineering of Saccharomyces cerevisiae for efficient anaerobic alcoholic fermentation of L-arabinose. *Appl. Environ. Microbiol. 73*, 4881–4891.

(4) Atsumi, S., Wu, T.-Y., Machado, I. M. P., Huang, W.-C., Chen, P.-Y., Pellegrini, M., and Liao, J. C. (2010) Evolution, genomic analysis, and reconstruction of isobutanol tolerance in Escherichia coli. *Mol. Syst. Biol. 6*, 449.

(5) Kwon, Y. D., Kim, S., Lee, S. Y., and Kim, P. (2011) Long-term continuous adaptation of Escherichia coli to high succinate stress and transcriptome analysis of the tolerant strain. *J. Biosci. Bioeng. 111*, 26–30.

(6) Fong, S. S., Burgard, A. P., Herring, C. D., Knight, E. M., Blattner, F. R., Maranas, C. D., and Palsson, B. O. (2005) In silico design and adaptive evolution of Escherichia coli for production of lactic acid. *Biotechnol. Bioeng. 91*, 643–648.

(7) Hu, H., and Wood, T. K. (2010) An evolved Escherichia coli strain for producing hydrogen and ethanol from glycerol. *Biochem. Biophys. Res. Commun. 391*, 1033–1038.

(8) Conrad, T. M., Joyce, A. R., Applebee, M. K., Barrett, C. L., Xie, B., Gao, Y., and Palsson, B. Ø. (2009) Whole-genome resequencing of Escherichia coli K-12 MG1655 undergoing short-term laboratory evolution in lactate minimal media reveals flexible selection of adaptive mutations. *Genome Biol. 10*, R118.

(9) Alper, H., Moxley, J., Nevoigt, E., Fink, G. R., and Stephanopoulos, G. (2006) Engineering Yeast Transcription Machinery for Improved Ethanol Tolerance and Production. *Science. 314*, 1565–1568.

(10) Wang, H. H., Isaacs, F. J., Carr, P. a, Sun, Z. Z., Xu, G., Forest, C. R., and Church, G. M. (2009) Programming cells by multiplex genome engineering and accelerated evolution. *Nature 460*, 894–898.

(11) Jiang, W., Bikard, D., Cox, D., Zhang, F., and Marraffini, L. a. (2013) RNA-guided editing of bacterial genomes using CRISPR-Cas systems. *Nat Biotechnol 31*, 233–239.

(12) Reyes, L. H., Gomez, J. M., and Kao, K. C. (2014) Improving carotenoids production in yeast via adaptive laboratory evolution. *Metab. Eng. 21*, 26–33.

(13) Yang, J., Seo, S. W., Jang, S., Shin, S.-I., Lim, C. H., Roh, T.-Y., and Jung, G. Y. (2013) Synthetic RNA devices to expedite the evolution of metabolite-producing microbes. *Nat. Commun. 4*, 1413.

(14) Raman, S., Rogers, J. K., Taylor, N. D., and Church, G. M. (2014) Evolution-guided optimization of biosynthetic pathways. *Proc. Natl. Acad. Sci. 111*, 17803–17808.

(15) Davies, J., and Davies, D. (2010) Origins and Evolution of Antibiotic Resistance.

Microbiol. Mol. Biol. Rev. 74, 417–433.
(16) Gong, F., and Yanofsky, C. (2002) Instruction of translating ribosome by nascent peptide. *Science. 297*, 1864–1867.
(17) Fang, M., Wang, T., Zhang, C., Bai, J., Zheng, X., Zhao, X., Lou, C., and Xing, X.-H. (2016) Intermediate-sensor assisted push-pull strategy and its application in heterologous deoxyviolacein production in Escherichia coli. *Metab. Eng. 33*, 41–51.
(18) Pugsley, A. P., and Dubreuil, C. (1988) Molecular characterization of malQ , the structural gene for the Escherichia coii enzyme amylomaltase. *Mol. Microbiol. 2*, 473–479.
(19) Fang, M.-Y., Zhang, C., Yang, S., Cui, J.-Y., Jiang, P.-X., Lou, K., Wachi, M., and Xing, X.-H. (2015) High crude violacein production from glucose by Escherichia coli engineered with interactive control of tryptophan pathway and violacein biosynthetic pathway. *Microb. Cell Fact. 14*, 8.
(20) Binder, S., Schendzielorz, G., Stäbler, N., Krumbach, K., Hoffmann, K., Bott, M., and Eggeling, L. (2012) A high-throughput approach to identify genomic variants of bacterial metabolite producers at the single-cell level. *Genome Biol. 13*, R40.
(21) Echols, H., Lu, C., and Burgers, P. M. (1983) Mutator strains of Escherichia coli, mutD and dnaQ, with defective exonucleolytic editing by DNA polymerase III holoenzyme. *Proc. Natl. Acad. Sci. U. S. A. 80*, 2189–2192.
(22) Fijalkowska, I. J., and Schaaper, R. M. (1996) Mutants in the Exo I motif of Escherichia coli dnaQ: defective proofreading and inviability due to error catastrophe. *Proc. Natl. Acad. Sci. U. S. A. 93*, 2856–2861.
(23) Zhang, X., Zhang, X.-F., Li, H.-P., Wang, L.-Y., Zhang, C., Xing, X.-H., and Bao, C.-Y. (2014) Atmospheric and room temperature plasma (ARTP) as a new powerful mutagenesis tool. *Appl. Microbiol. Biotechnol. 98*, 5387–5396.
(24) Walsh, C. (2000) Molecular mechanisms that confer antibacterial drug resistance. *Nature 406*, 775–781.
(25) Chopra, I., and Roberts, M. (2001) Tetracycline Antibiotics: Mode of Action, Applications, Molecular Biology, and Epidemiology of Bacterial Resistance. *Microbiol. Mol. Biol. Rev. 65*, 232–260.
(26) Aminov, R. I., and Mackie, R. I. (2001) Molecular Ecology of Tetracycline Resistance: Development and Validation of Primers for Detection of Tetracycline Resistance Genes Encoding Ribosomal Protection Proteins. *Appl. Environ. Microbiol. 67*, 22–32.
(27) Schnappinger, D., and Hillen, W. (1996) Tetracyclines: Antibiotic action, uptake, and resistance mechanisms. *Arch. Microbiol. 165*, 359–369.
(28) George, A. M., and Levy, S. B. (1983) Gene in the major cotransduction gap of the Escherichia coli K-12 linkage map required for the expression of chromosomal resistance to tetracycline and other antibiotics. *J. Bacteriol. 155*, 541–548.
(29) Okusu, H., Ma, D., and Nikaido, H. (1996) AcrAB Efflux Pump Plays a Major Role in the Antibiotic Resistance Phenotype of Escherichia coli Multiple-Antibiotic-Resistance (Mar) Mutants. *J. Bacteriol. 178*, 306–308.
(30) Chollet, R., Chevalier, J., Bryskier, A., and Pagès, J. M. (2004) The AcrAB-TolC pump is involved in macrolide resistance but not in telithromycin efflux in

Enterobacter aerogenes and Escherichia coli. *Antimicrob. Agents Chemother. 48*, 3621–3624.
(31) de Cristóbal, R. E., Vincent, P. a., and Salomón, R. a. (2006) Multidrug resistance pump AcrAB-TolC is required for high-level, Tet(A)-mediated tetracycline resistance in Escherichia coli. *J. Antimicrob. Chemother. 58*, 31–36.
(32) Paulsen, I. T., Brown, M. H., and Skurray, R. A. (1996) Proton-dependent multidrug efflux systems. *Microbiol. Rev. 60*, 575–608.
(33) Bolhuis, H., Van Veen, H. W., Poolman, B., Driessen, A. J. M., and Konings, W. N. (1997) Mechanisms of multidrug transporters. *FEMS Microbiol. Rev. 21*, 55–84.
(34) Cohen, S. P., McMurry, L. M., Hooper, D. C., Wolfson, J. S., and Levy, S. B. (1989) Cross-resistance to fluoroquinolones in multiple-antibiotic-resistant (Mar) Escherichia coli selected by tetracycline or chloramphenicol: Decreased drug accumulation associated with membrane changes in addition to OmpF reduction. *Antimicrob. Agents Chemother. 33*, 1318–1325.
(35) Cocozaki, A. I., Altman, R. B., Huang, J., Buurman, E. T., Kazmirski, S. L., Doig, P., Prince, D. B., Blanchard, S. C., Cate, J. H. D., and Ferguson, A. D. (2016) Resistance mutations generate divergent antibiotic susceptibility profiles against translation inhibitors. *Proc. Natl. Acad. Sci. 113*, 8188–8193.
(36) Blair, J. M., Richmond, G. E., and Piddock, L. J. (2014) Multidrug efflux pumps in Gram-negative bacteria and their role in antibiotic resistance. *Future Microbiol. 9*, 1165–1177.
(37) Boos, W., and Shuman, H. (1998) Maltose/Maltodextrin System of Escherichia coli: Transport, Metabolism, and Regulation. *Microbiol. Mol. Biol. Rev. 62*, 204–229.
(38) Schlegel, A., Böhm, A., Lee, S.-J., Peist, R., Decker, K., and Boos, W. (2002) Network regulation of the Escherichia coli maltose system. *J. Mol. Microbiol. Biotechnol. 4*, 301–307.
(39) Park, J. T., Shim, J. H., Tran, P. L., Hong, I. H., Yong, H. U., Oktavina, E. F., Nguyen, H. D., Kim, J. W., Lee, T. S., Park, S. H., Boos, W., and Park, K. H. (2011) Role of maltose enzymes in glycogen synthesis by Escherichia coli. *J. Bacteriol. 193*, 2517–2526.
(40) Janeček, Š., and Gabriško, M. (2016) Remarkable evolutionary relatedness among the enzymes and proteins from the α-amylase family. *Cell. Mol. Life Sci. 73*, 2707–2725.
(41) Mills, D. R., Peterson, R. L., and Spiegelman, S. (1967) An extracellular Darwinian experiment with a self-duplicating nucleic acid molecule. *Proc. Natl. Acad. Sci. U. S. A. 58*, 217–224.
(42) Wright, M. C., and Joyce, G. F. (1997) Continuous in Vitro Evolution of Catalytic Function. *Science (80-.). 276*, 614–617.
(43) Esvelt, K. M., Carlson, J. C., and Liu, D. R. (2011) A system for the continuous directed evolution of biomolecules. *Nature 472*, 499–503.
(44) Carlson, J. C., Badran, A. H., Guggiana-Nilo, D. A., and Liu, D. R. (2014) Negative selection and stringency modulation in phage-assisted continuous evolution. *Nat. Chem. Biol. 10*, 216–222.
(45) Hubbard, B. P., Badran, A. H., Zuris, J. a, Guilinger, J. P., Davis, K. M., Chen, L.,

Tsai, S. Q., Sander, J. D., Joung, J. K., and Liu, D. R. (2015) Continuous directed evolution of DNA-binding proteins to improve TALEN specificity. *Nat. Methods 12*, 939–942.

(46) Badran, A. H., Guzov, V. M., Huai, Q., Kemp, M. M., Vishwanath, P., Kain, W., Evdokimov, A., Moshiri, F., Turner, K. H., Wang, P., Malvar, T., and Liu, D. R. (2016) Continuous evolution of B . thuringiensis toxins overcomes Bt resistance in insects. *Nature 533*, 58–63.

(47) Crook, N., Abatemarco, J., Sun, J., Wagner, J. M., Schmitz, A., and Alper, H. S. (2016) In vivo continuous evolution of genes and pathways in yeast. *Nat. Commun. 7*, 13051.

(48) Spraggon, G., Kim, C., Nguyen-Huu, X., Yee, M. C., Yanofsky, C., and Mills, S. E. (2001) The structures of anthranilate synthase of Serratia marcescens crystallized in the presence of (i) its substrates, chorismate and glutamine, and a product, glutamate, and (ii) its end-product inhibitor, L-tryptophan. *Proc. Natl. Acad. Sci. U. S. A. 98*, 6021–6026.

(49) Xiao, Y., Bowen, C. H., Liu, D., and Zhang, F. (2016) Exploiting non-genetic cell-to-cell variation for enhanced biosynthesis. *Nat. Chem. Biol.* 12, 339–344.

(50) Zhang, X., Jantama, K., Moore, J. C., Jarboe, L. R., Shanmugam, K. T., and Ingram, L. O. (2009) Metabolic evolution of energy-conserving pathways for succinate production in Escherichia coli. *Proc. Natl. Acad. Sci. U. S. A. 106*, 20180–20185.

(51) Baba, T., Ara, T., Hasegawa, M., Takai, Y., Okumura, Y., Baba, M., Datsenko, K. A., Tomita, M., Wanner, B. L., and Mori, H. (2006) Construction of Escherichia coli K-12 in-frame, single-gene knockout mutants: the Keio collection. *Mol. Syst. Biol. 2*, 2006.0008.

(52) Sack, J. S., Kish, K. F., Pokross, M., Xie, D., Duke, G. J., Tredup, J. A., … Newitt, J. A. (2008) Structural basis for the high-affinity binding of pyrrolotriazine inhibitors of p38 MAP kinase. *Acta Crystallogr. Sect. D Biol. Crystallogr. 64*, 705–710.

(53) Arnold, F. H. (2003) Directed Evolution Library Creation Edited by. *Hum. Press Inc. 231*, 3,29.

(54) Gibson, D. G., Young, L., Chuang, R.-Y., Venter, J. C., Hutchison, C. A., and Smith, H. O. (2009) Enzymatic assembly of DNA molecules up to several hundred kilobases. *Nat. Methods 6*, 343–345.

(55) Stewart, V. (2008) The ribosome: a metabolite-responsive transcription regulator. *J. Bacteriol. 190*, 4787–4790.

(56) Moon, T. S., Lou, C., Tamsir, A., Stanton, B. C., and Voigt, C. a. (2012) Genetic programs constructed from layered logic gates in single cells. *Nature 491*, 249–253.

Figure 1a

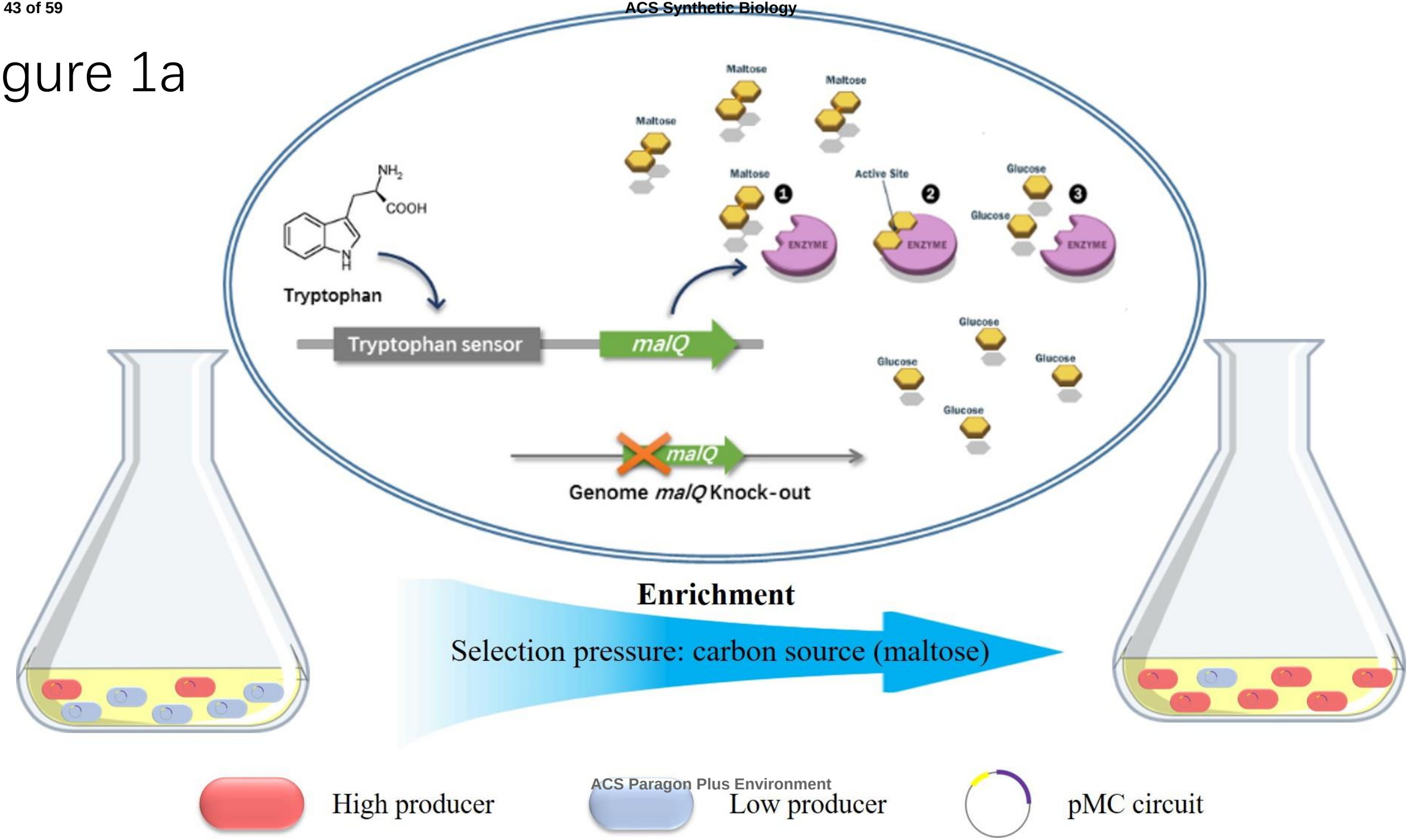
Maltose
Maltose
Maltose
Maltose
Active Site
Glucose
Glucose
ENZYME
ENZYME
ENZYME
1
2
3
NH2
COOH
Tryptophan
Tryptophan sensor
malQ
Glucose
Glucose
Glucose
Glucose
malQ
Genome malQ Knock-out
Enrichment
Selection pressure: carbon source (maltose)
High producer
Low producer
pMC circuit

Figure 1b

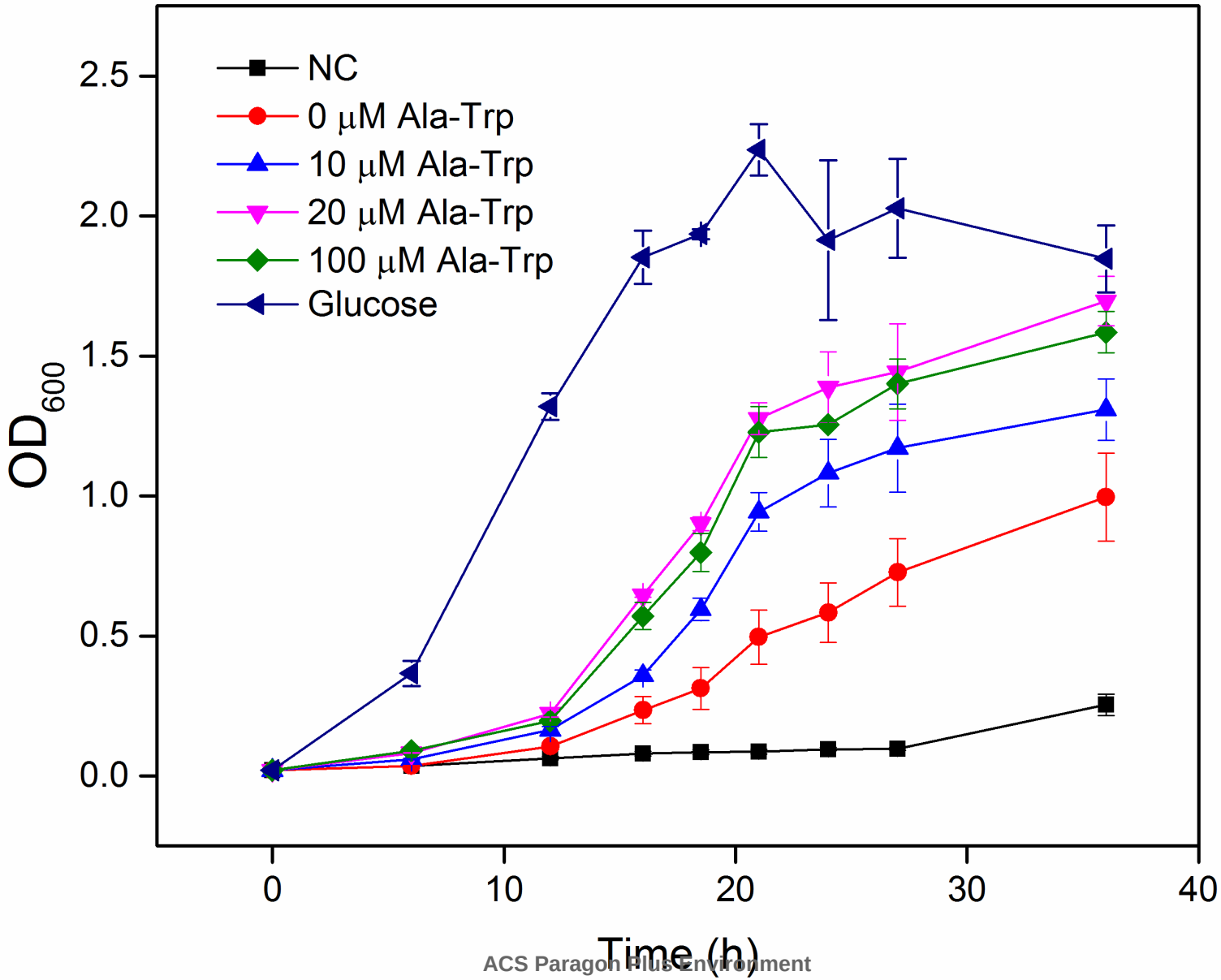
NC
0 μM Ala-Trp
10 μM Ala-Trp
20 μM Ala-Trp
100 μM Ala-Trp
Glucose
OD600
Time (h)
0.0
0.5
1.0
1.5
2.0
2.5
0
10
20
30
40

Figure 1c

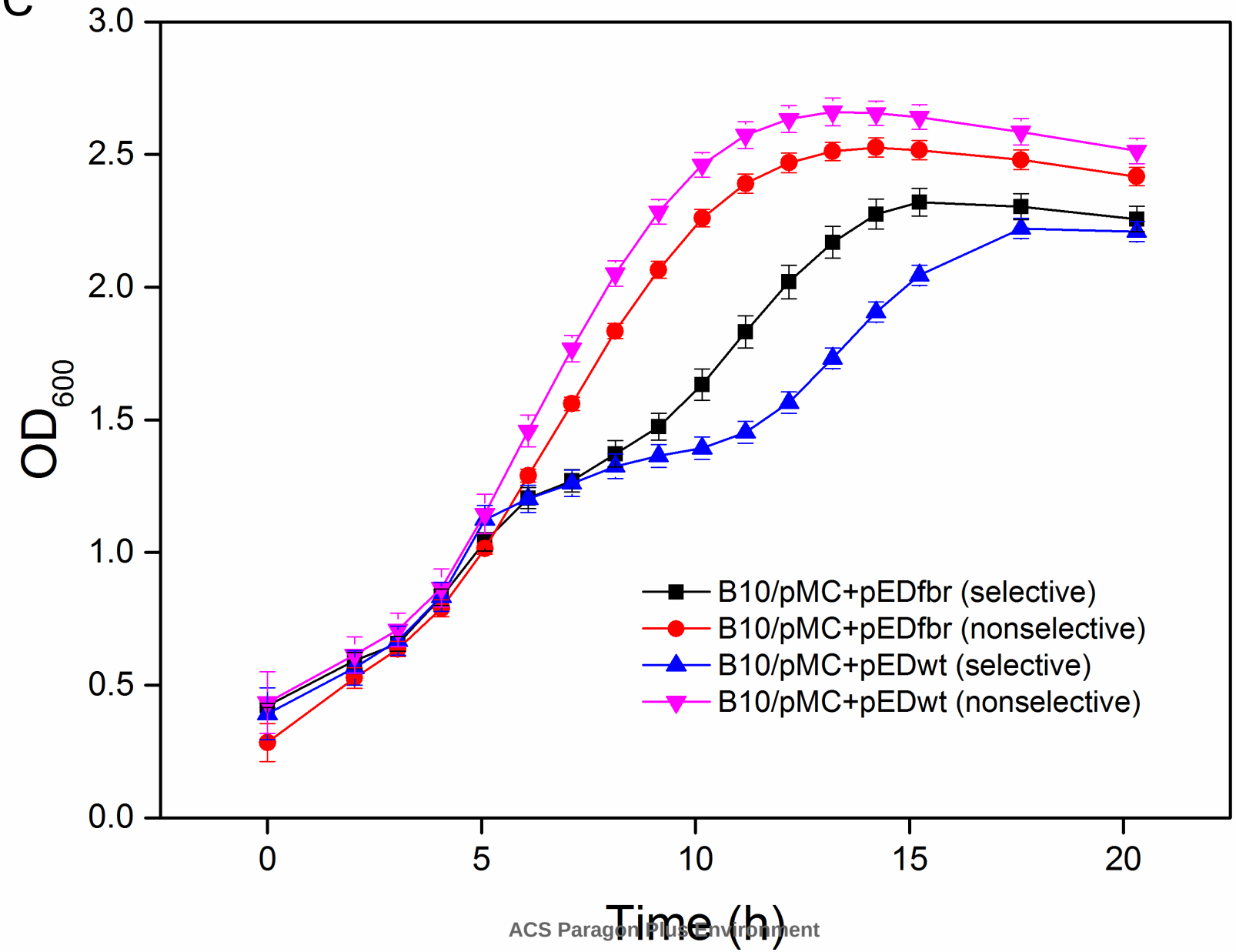

Figure 1d

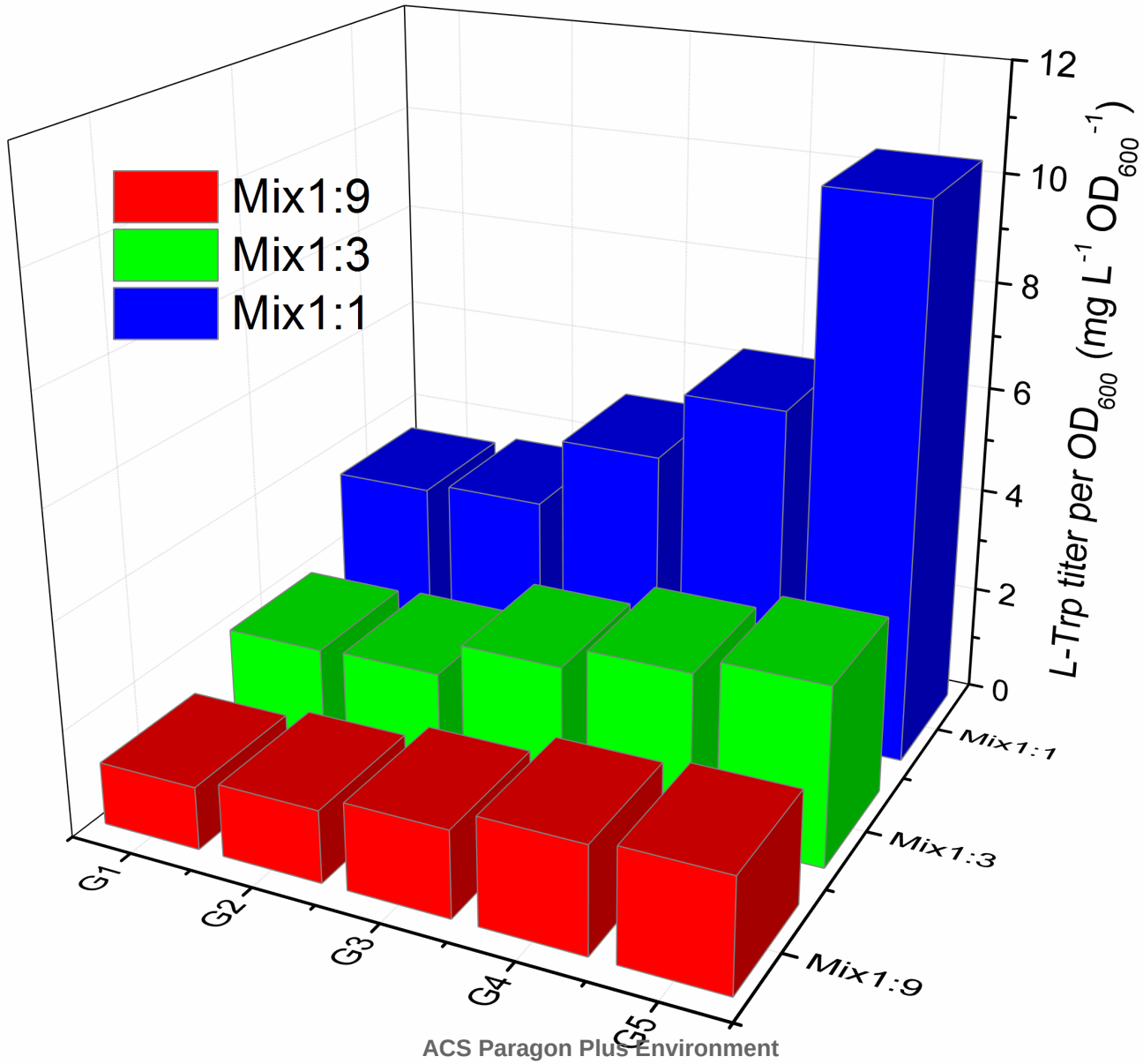
Mix1:9
Mix1:3
Mix1:1
12
10
8
6
4
2
0
L-Trp titer per OD600 (mg L-1 OD600-1)
G1
G2
G3
G4
G5
Mix1:1
Mix1:3
Mix1:9

Figure 2a

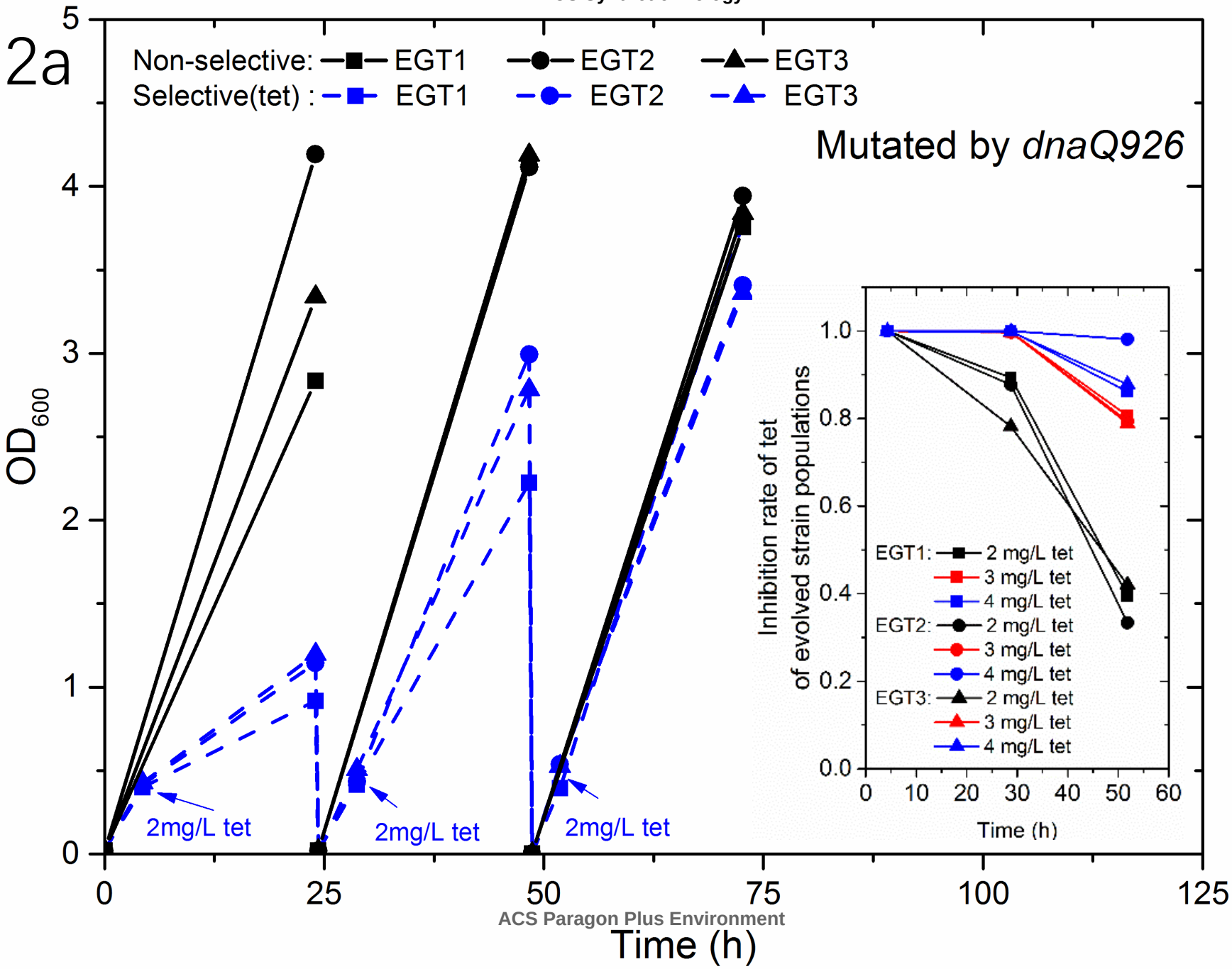
Non-selective: EGT1 EGT2 EGT3
Selective(tet) : EGT1 EGT2 EGT3
Mutated by dnaQ926
OD600
Time (h)
2mg/L tet
2mg/L tet
2mg/L tet
Inhibition rate of tet of evolved strain populations
EGT1: 2 mg/L tet
3 mg/L tet
4 mg/L tet
EGT2: 2 mg/L tet
3 mg/L tet
4 mg/L tet
EGT3: 2 mg/L tet
3 mg/L tet
4 mg/L tet
Time (h)

Figure 2b

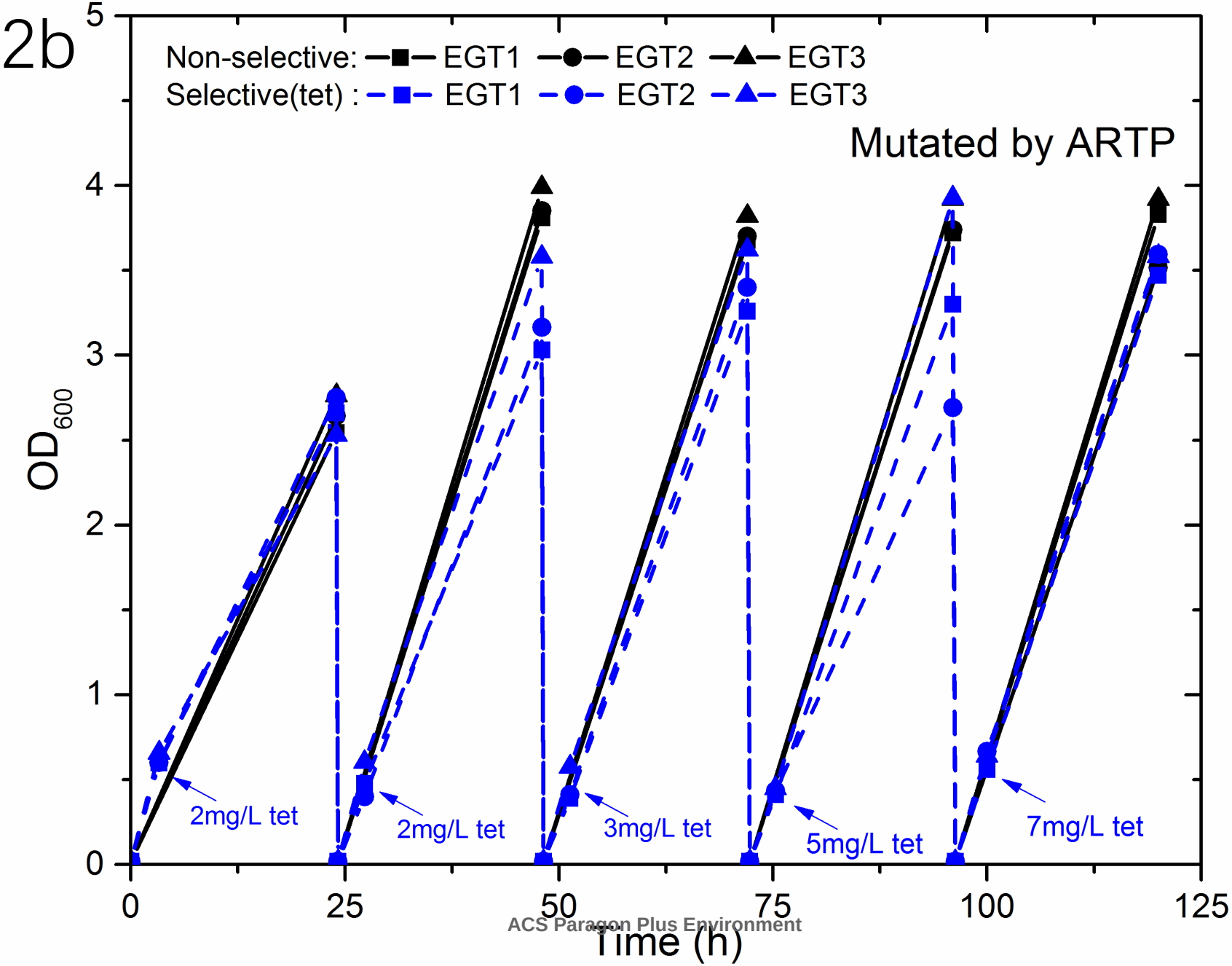

Figure 2c

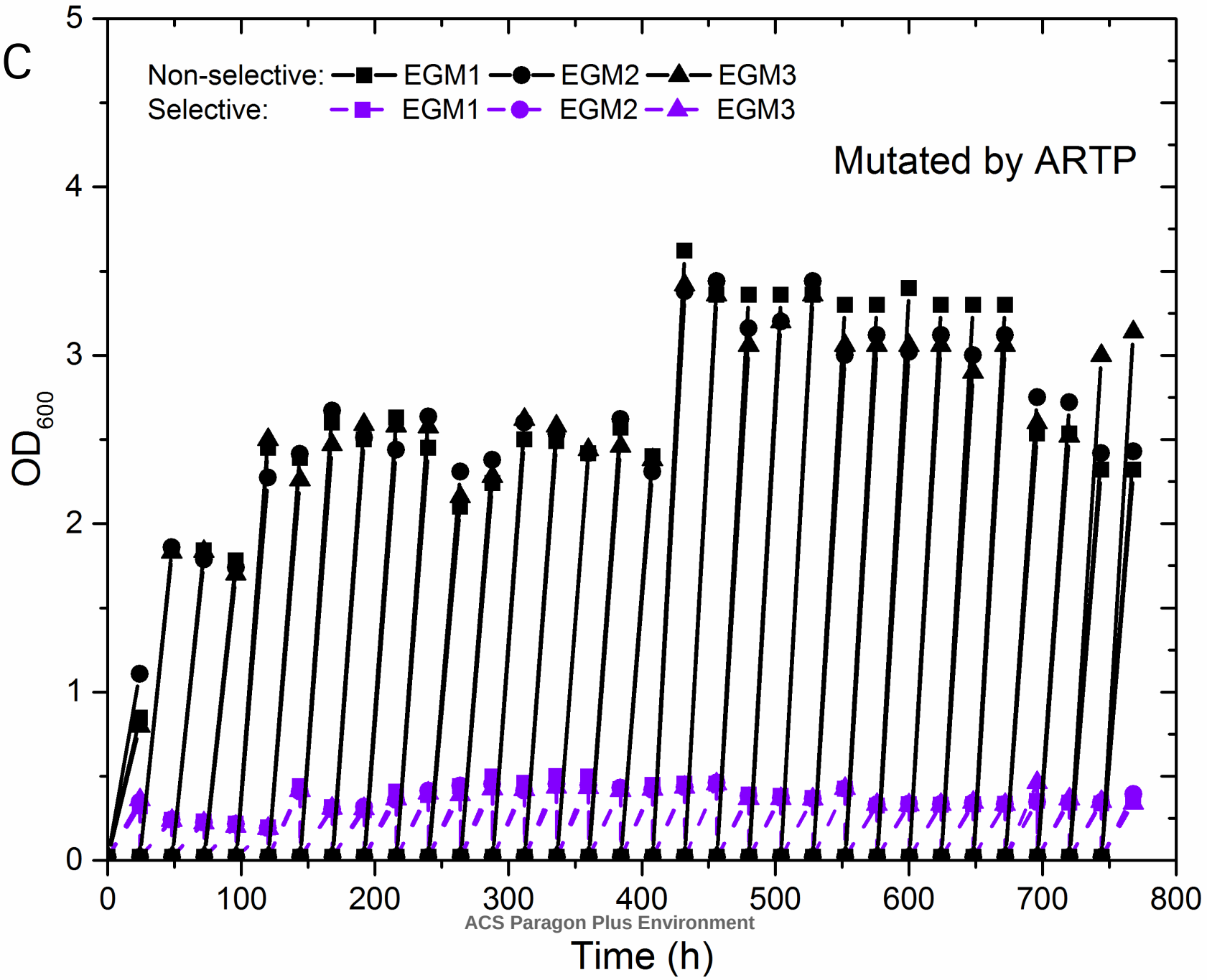

Figure 3a

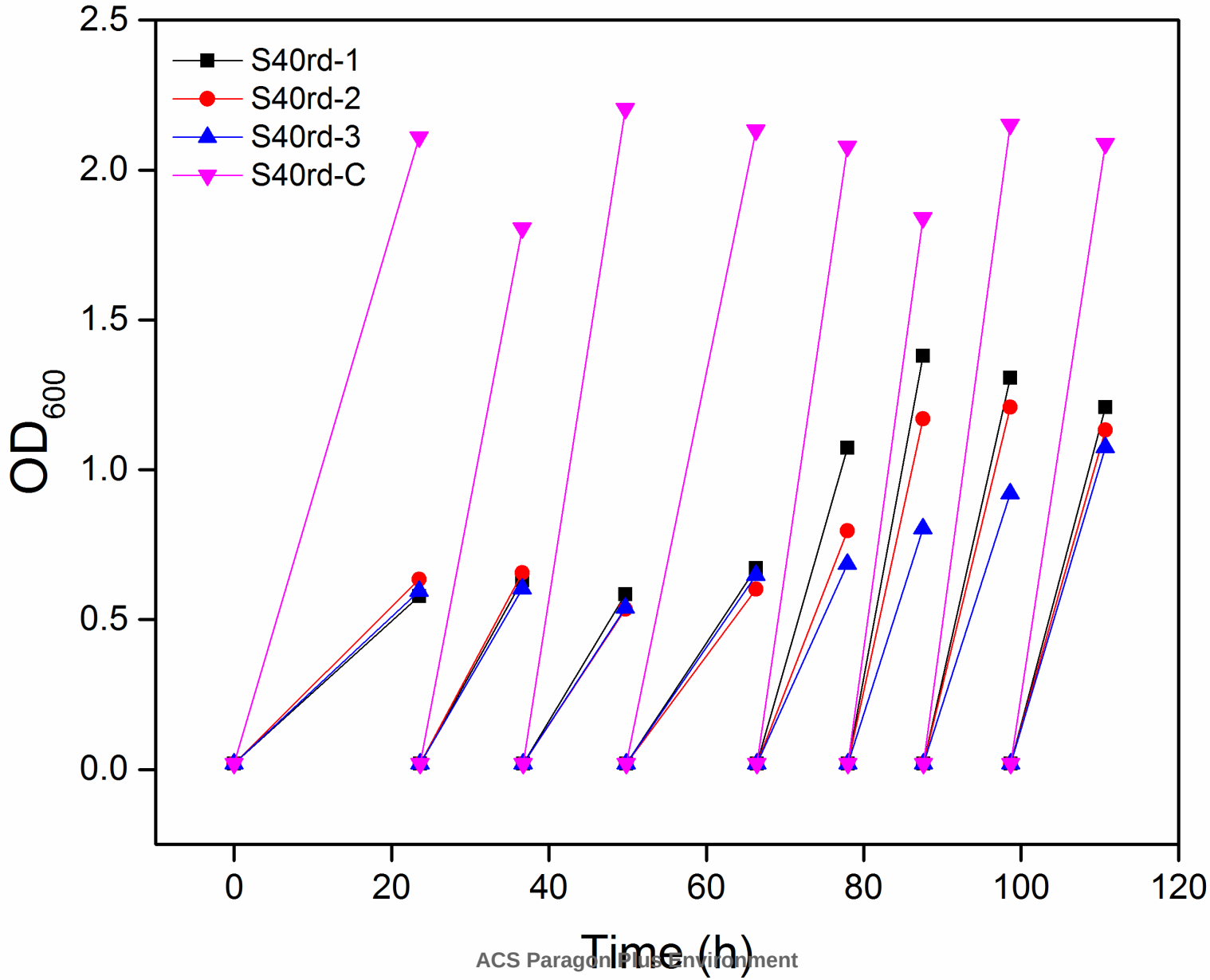

Figure 3b

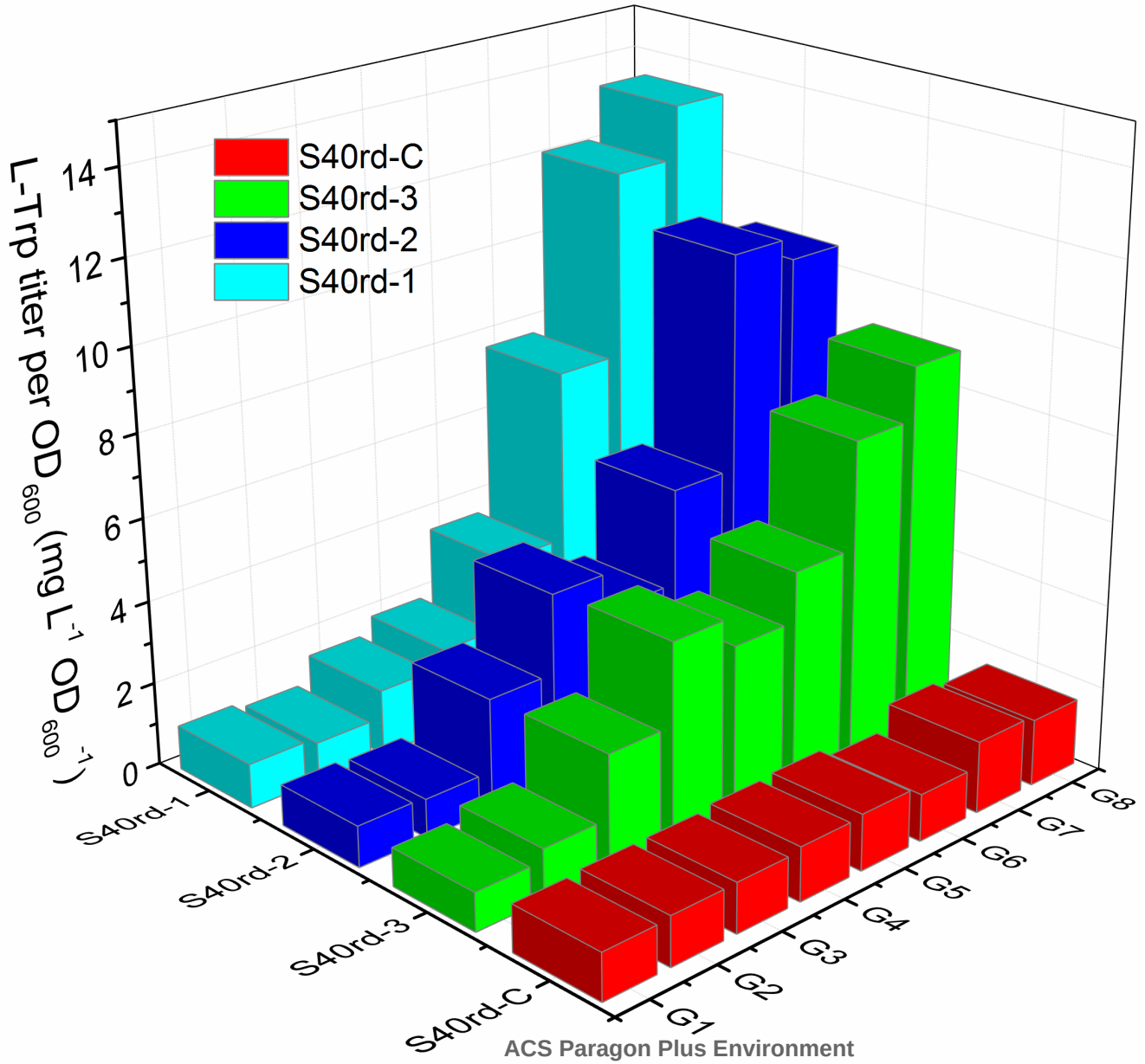
S40rd-C
S40rd-3
S40rd-2
S40rd-1
L-Trp titer per OD600 (mg L-1 OD600-1)
0
2
4
6
8
10
12
14
S40rd-1
S40rd-2
S40rd-3
S40rd-C
G1
G2
G3
G4
G5
G6
G7
G8
ACS Paragon Plus Environment

Figure 3c

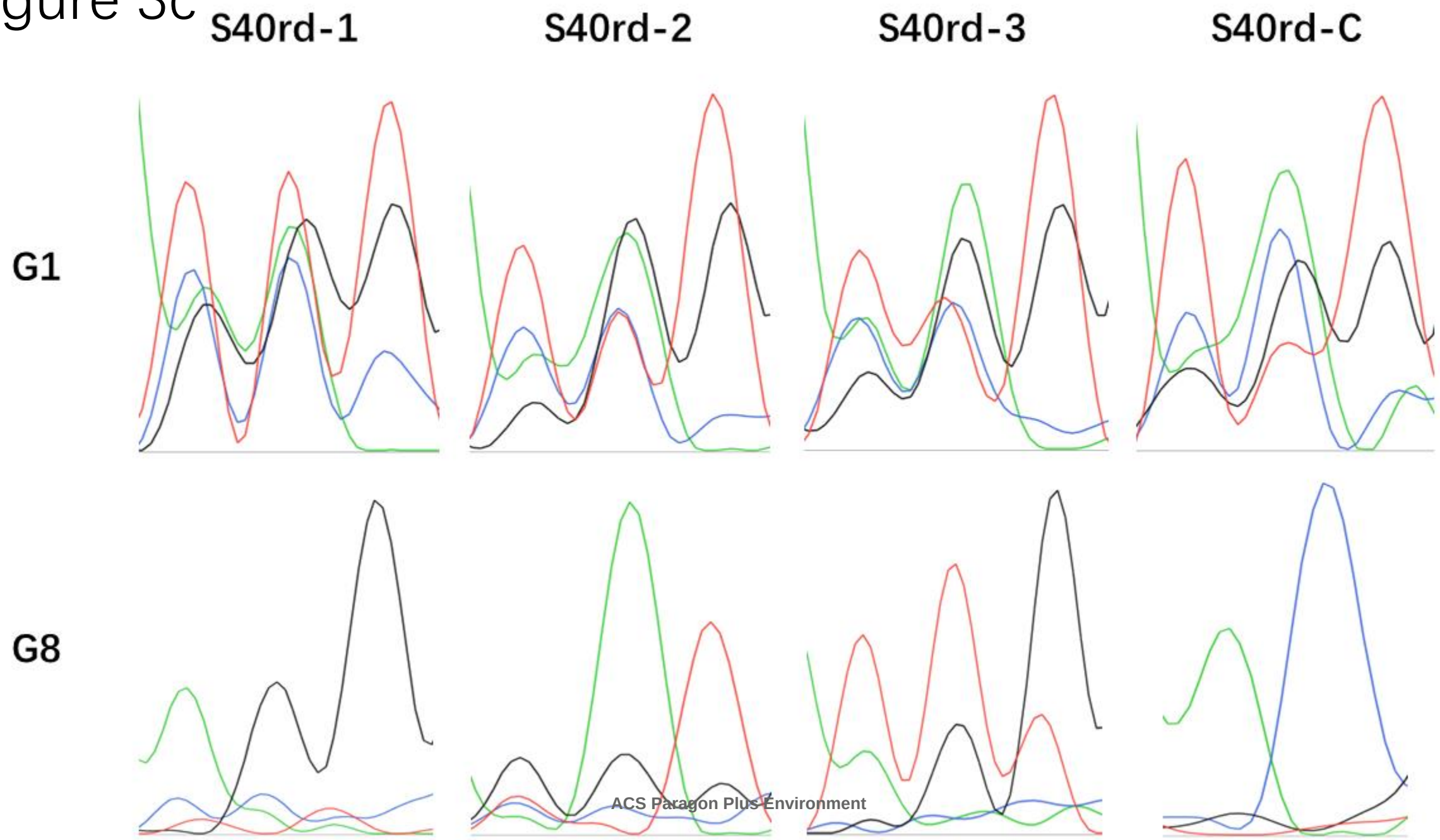

Figure 3d

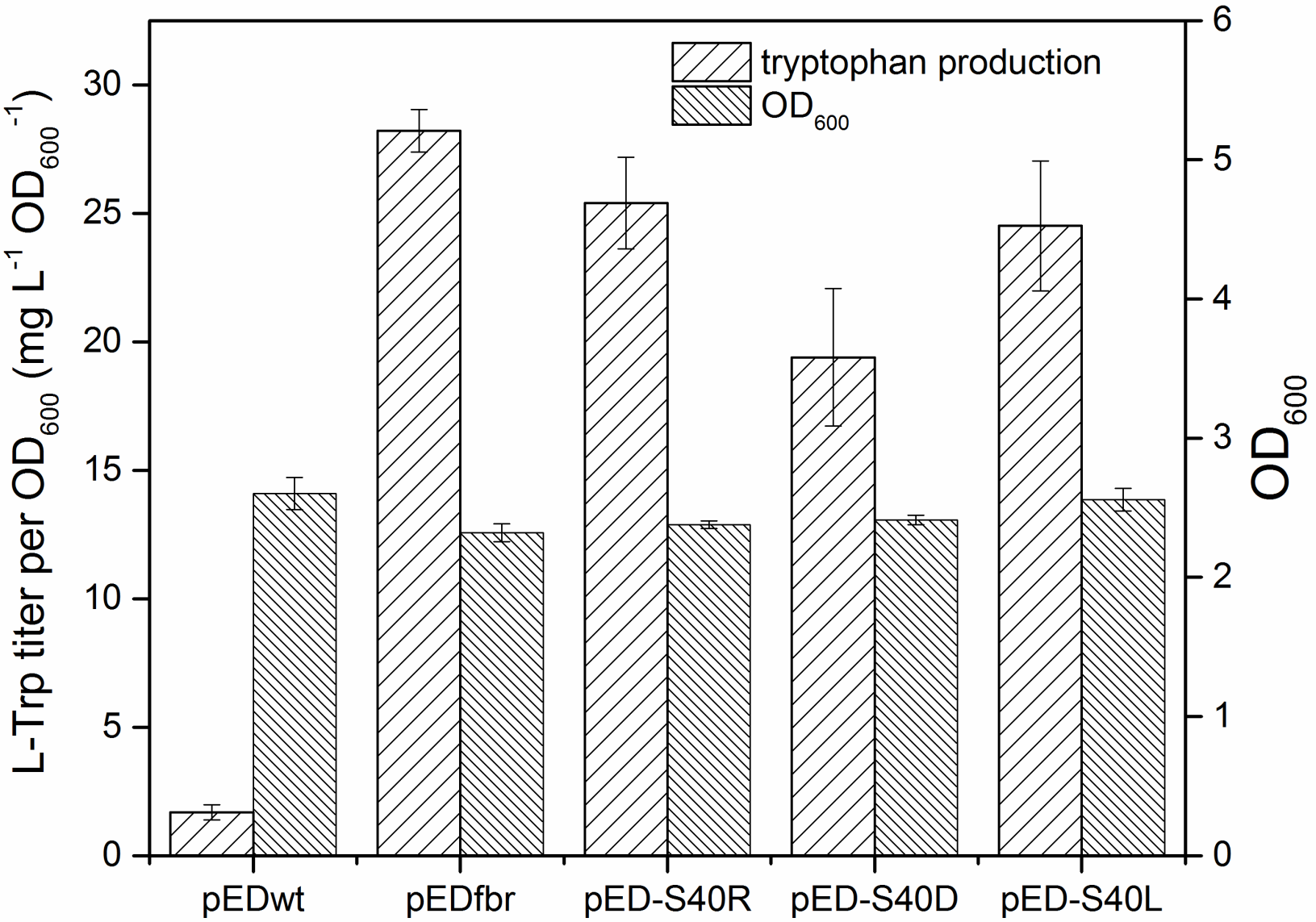
tryptophan production
OD600
L-Trp titer per OD600 (mg L-1 OD600-1)
OD600
0
5
10
15
20
25
30
0
1
2
3
4
5
6
pEDwt
pEDfbr
pED-S40R
pED-S40D
pED-S40L

Figure 4a

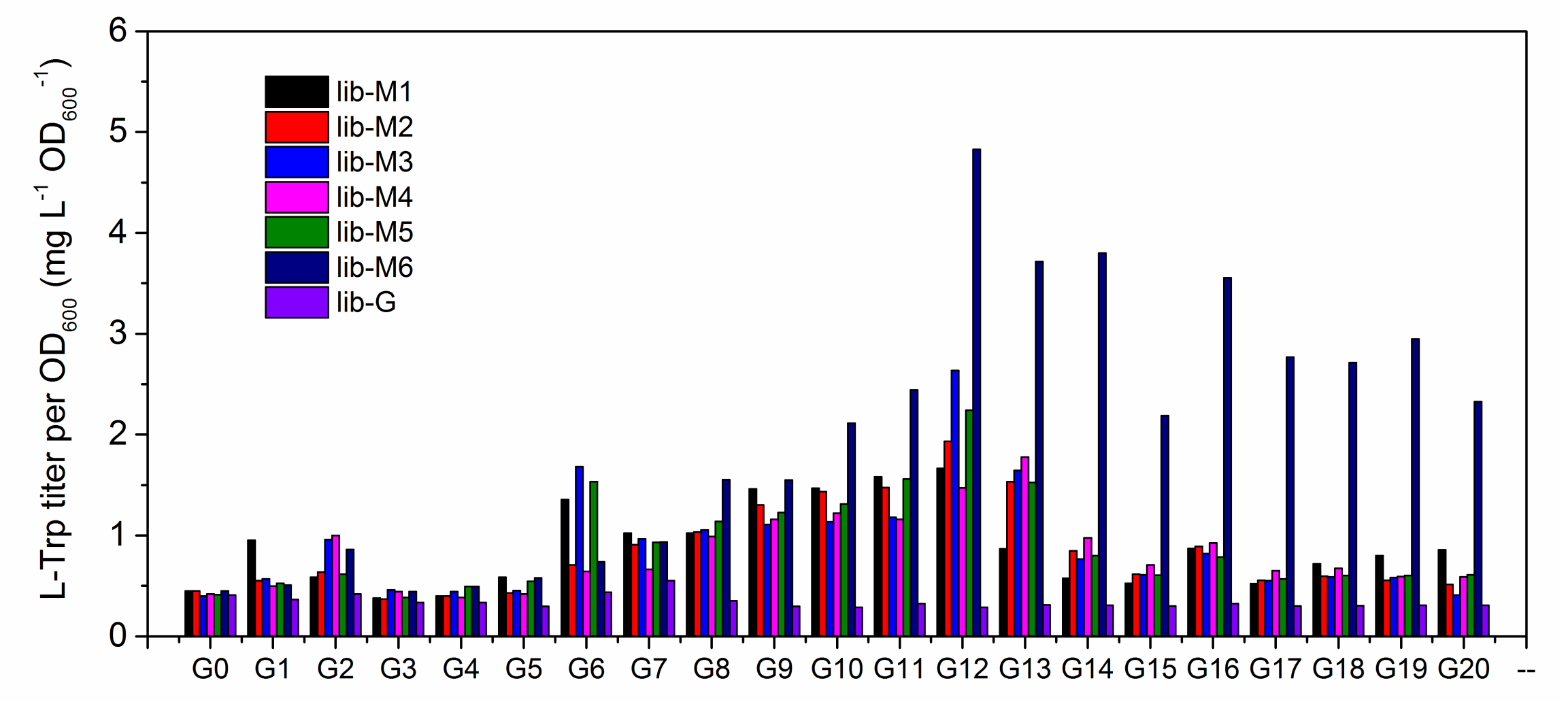
L-Trp titer per OD600 (mg L-1 OD600-1)
0
1
2
3
4
5
6
lib-M1
lib-M2
lib-M3
lib-M4
lib-M5
lib-M6
lib-G
G0
G1
G2
G3
G4
G5
G6
G7
G8
G9
G10
G11
G12
G13
G14
G15
G16
G17
G18
G19
G20
--

Figure 4b

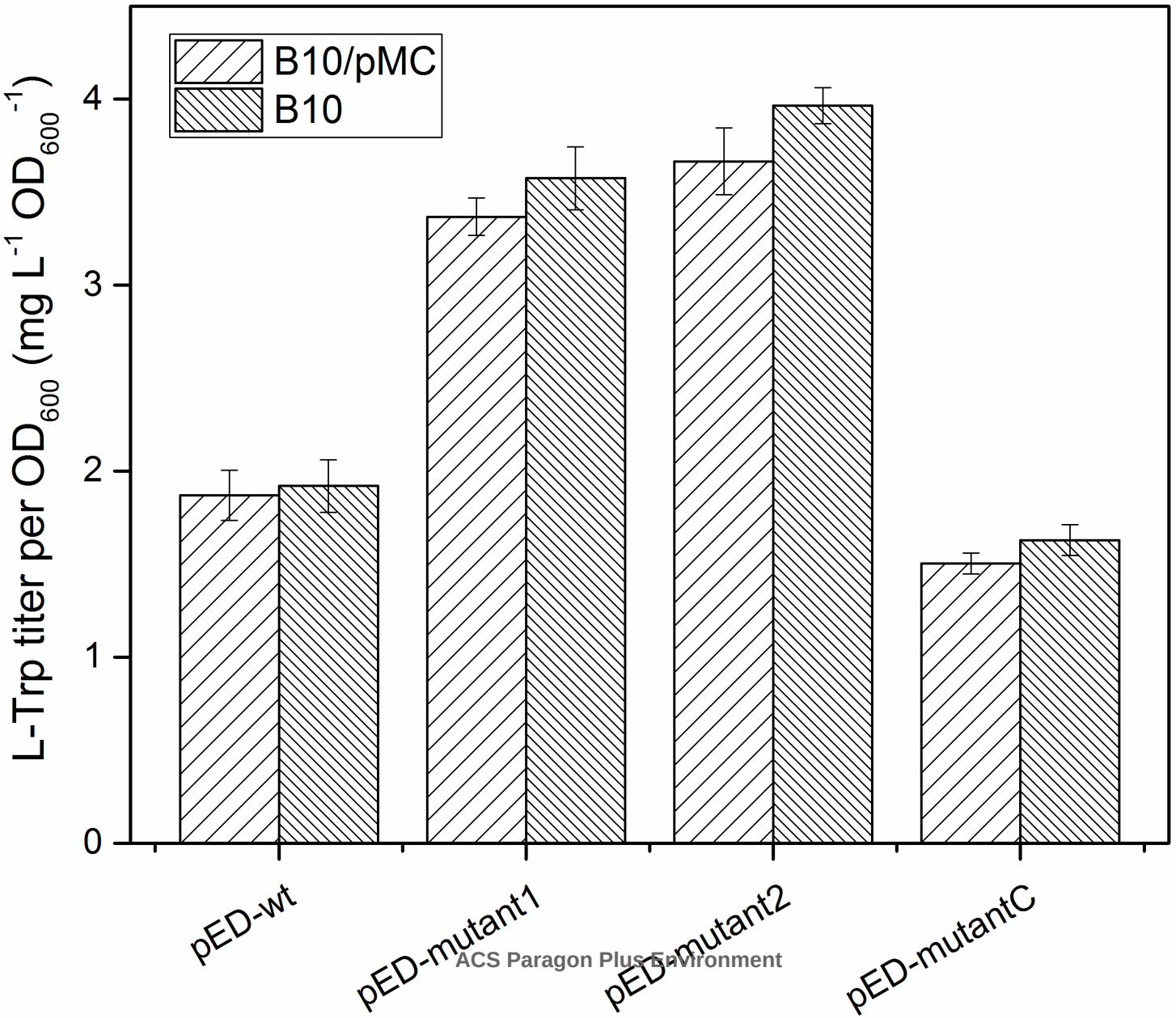

Figure 5a

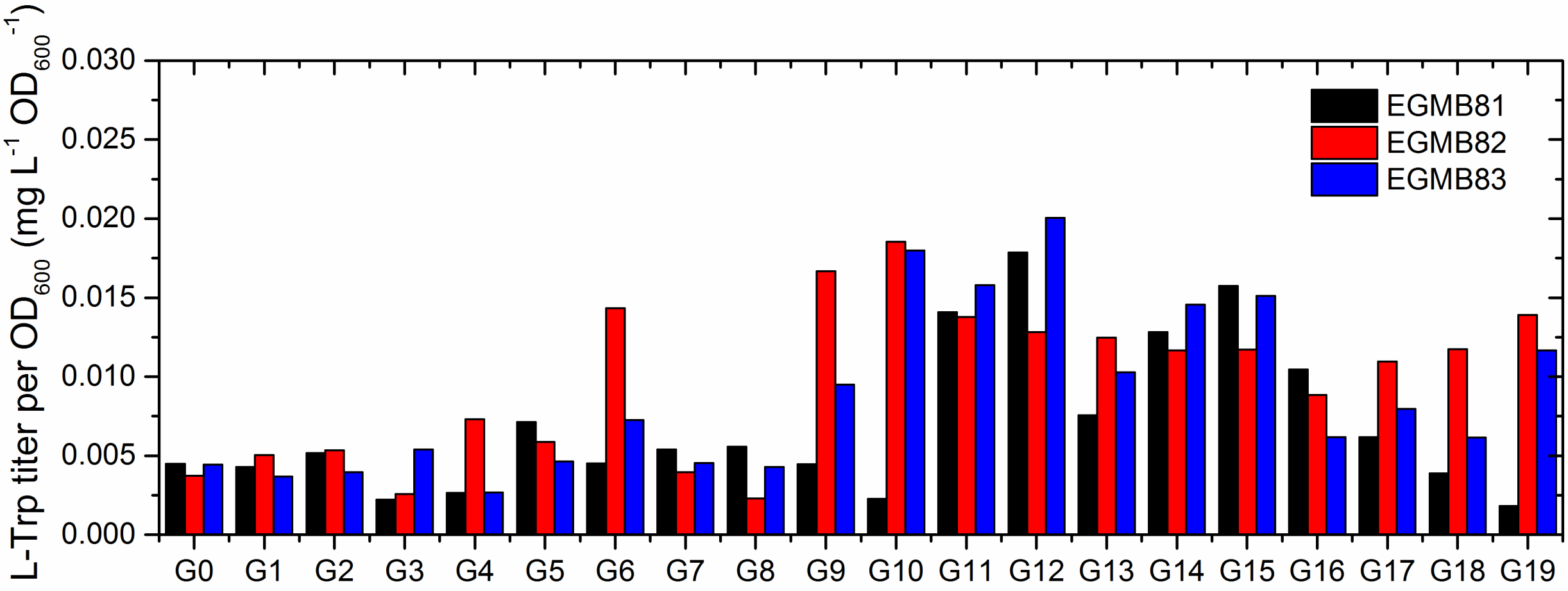
L-Trp titer per OD600 (mg L-1 OD600-1)
0.030
0.025
0.020
0.015
0.010
0.005
0.000
EGMB81
EGMB82
EGMB83
G0
G1
G2
G3
G4
G5
G6
G7
G8
G9
G10
G11
G12
G13
G14
G15
G16
G17
G18
G19

Figure 5b

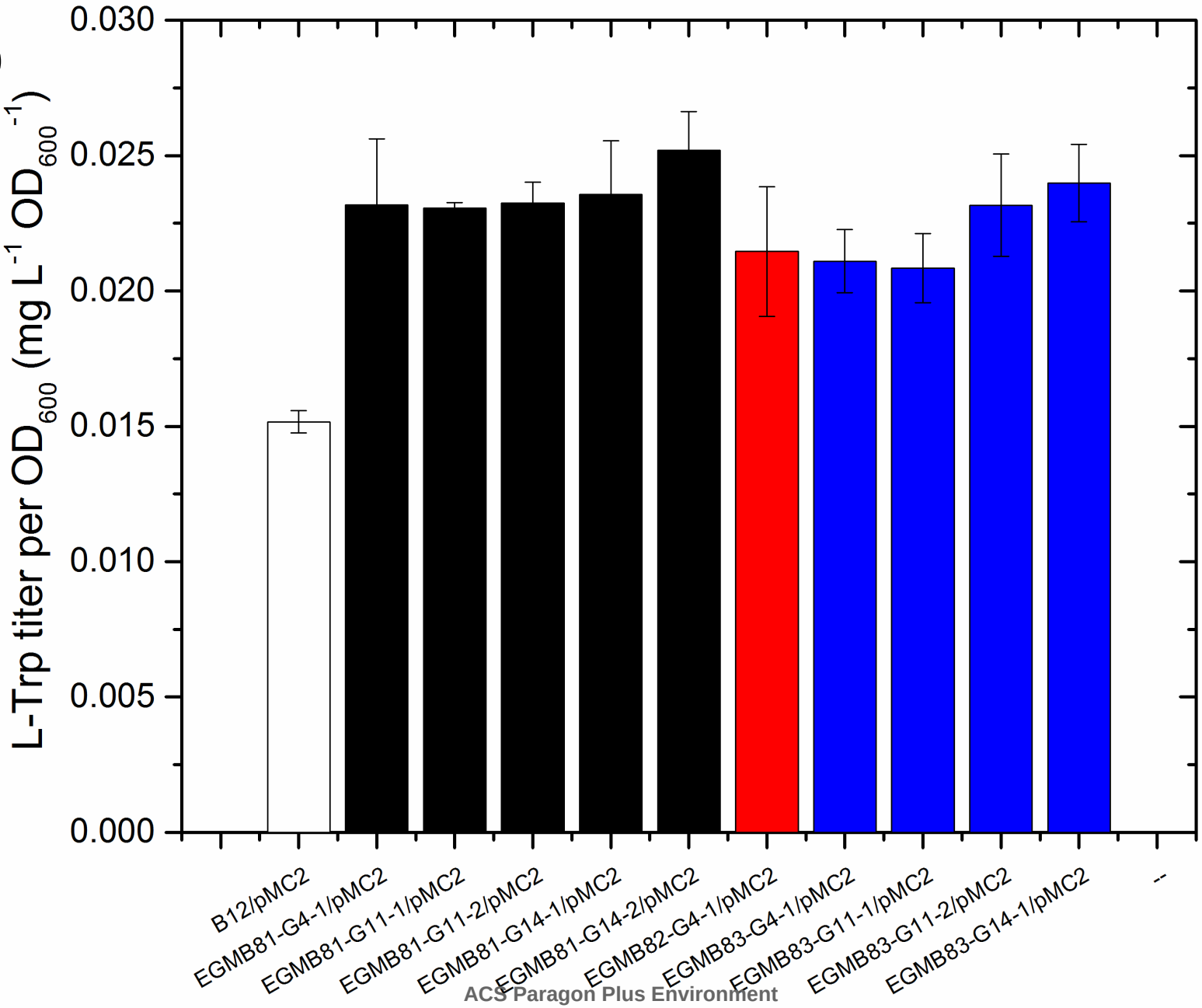
L-Trp titer per OD600 (mg L-1 OD600-1)
0.030
0.025
0.020
0.015
0.010
0.005
0.000
B12/pMC2
EGMB81-G4-1/pMC2
EGMB81-G11-1/pMC2
EGMB81-G11-2/pMC2
EGMB81-G14-1/pMC2
EGMB81-G14-2/pMC2
EGMB82-G4-1/pMC2
EGMB83-G4-1/pMC2
EGMB83-G11-1/pMC2
EGMB83-G11-2/pMC2
EGMB83-G14-1/pMC2
--

For Table of Contents Use Only

Maltose Utilization as a Novel Selection Strategy for Continuous Evolution of Microbes with Enhanced Metabolite Production

Shu-De Liu[1,2], Yi-Nan Wu[1,2], Tian-Min Wang, Chong Zhang*[,1], Xin-Hui Xing[1]

[1]MOE Key Laboratory for Industrial Biocatalysis, Department of Chemical Engineering, Center for Synthetic & Systems Biology, Tsinghua University, Beijing, China

[2]These authors contributed equally to the work

*Corresponding author, Chong Zhang: chongzhang@tsinghua.edu.cn

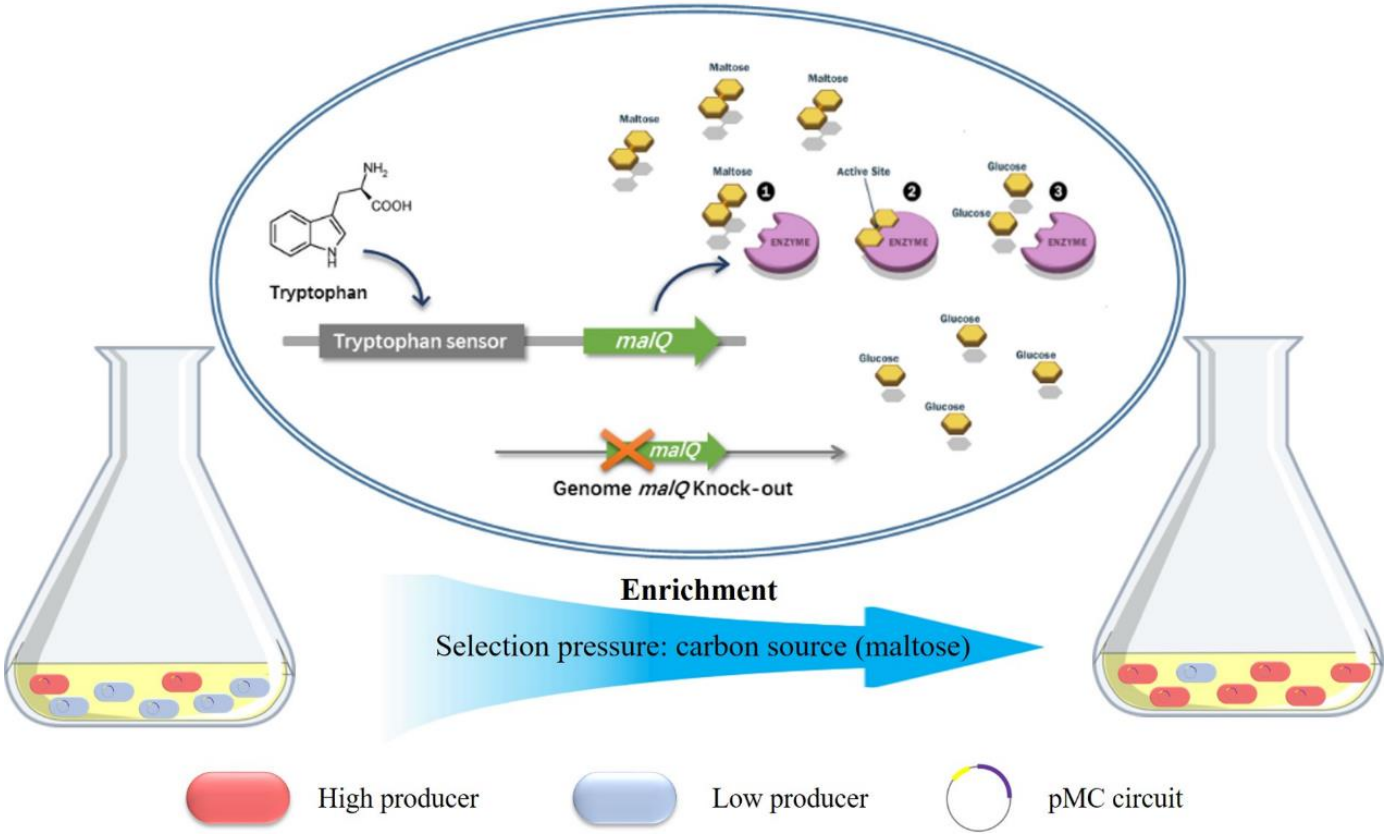

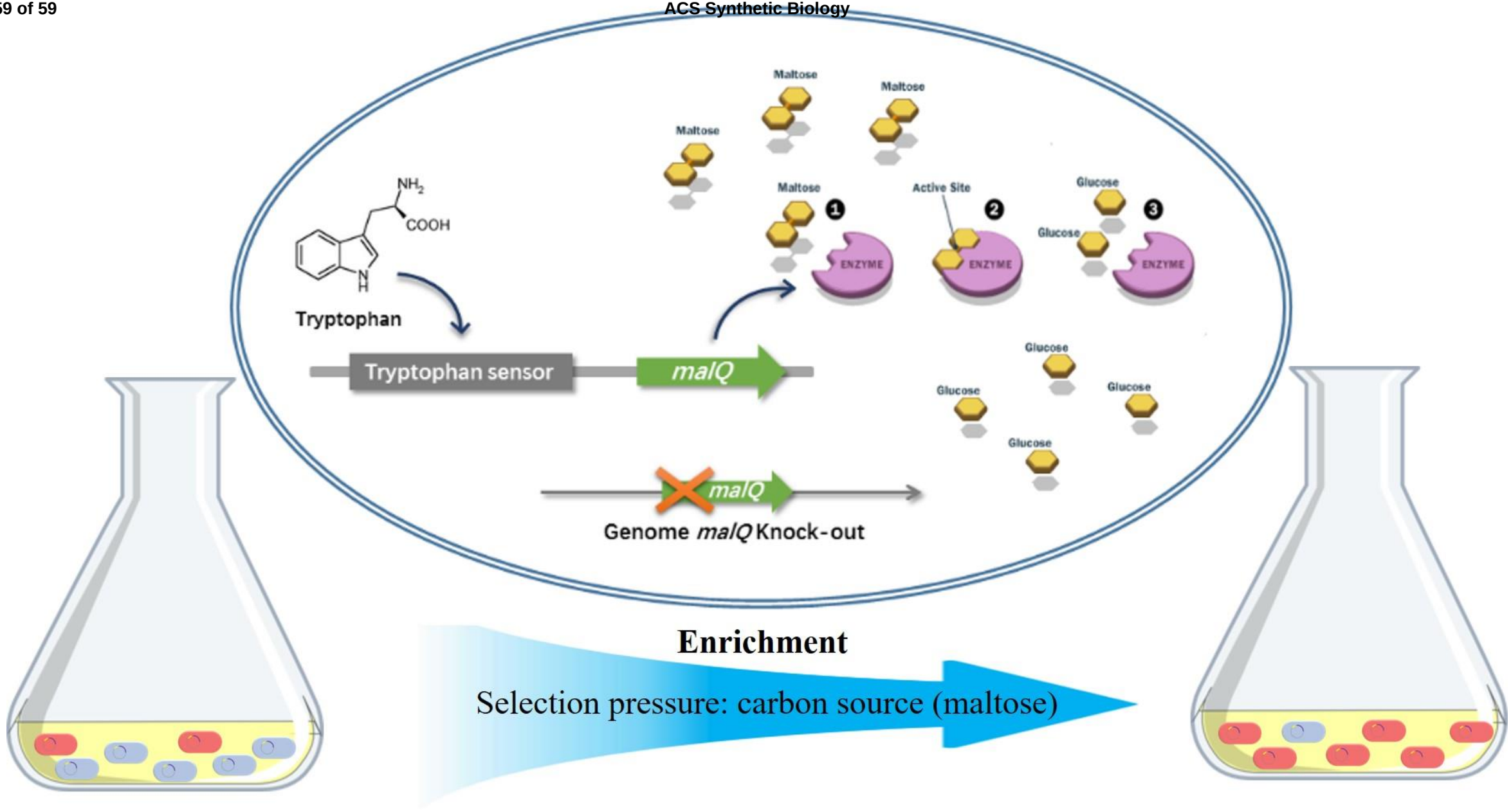
Maltose
Maltose
Maltose
Maltose
Active Site
Glucose
Glucose
ENZYME
ENZYME
ENZYME
1
2
3
NH2
COOH
Tryptophan
Tryptophan sensor
malQ
Glucose
Glucose
Glucose
Glucose
malQ
Genome malQ Knock-out
Enrichment
Selection pressure: carbon source (maltose)
High producer
Low producer
pMC circuit